ADVANCED DIAGNOSTIC MODALITIES AND MINIMALLY INVASIVE APPROACHES IN PEDIATRIC RADIOLOGY: A MULTIDISCIPLINARY REFERENCE

Edited by
Assist. Prof. Dr. Büşra ŞEKER

Specialist Dr. Hasan GENÇ
Specialist Dr. Melike YEŞİLDAL
Specialist Dr. Ali CANTÜRK
Lecturer Dr. Ayşe ARI
Assist. Prof. Dr. Büşra ŞEKER

ISBN 978-625-5753-51-9
Ankara -2025

ADVANCED DIAGNOSTIC MODALITIES AND MINIMALLY INVASIVE APPROACHES IN PEDIATRIC RADIOLOGY: A MULTIDISCIPLINARY REFERENCE

EDITOR

Assist. Prof. Dr. Büşra ŞEKER
busrasoylu.obs@gmail.com
ORCID ID: 0000-0001-7766-4276

AUTHORS

Specialist Dr. Hasan GENÇ[1]

Specialist Dr. Melike YEŞİLDAL[2]

Specialist Dr. Ali CANTÜRK[3]

Lecturer Dr. Ayşe ARI[4]

Assist. Prof. Dr. Büşra ŞEKER[5]

[1]Fethi Sekin City Hospital, Department of Radiology, Elazığ, Türkiye
dr.hsngnc@gmail.com
ORCID ID: 0009-0002-6366-3146

[2]Abdulhamid Han Resarch Hospital Interventional Radiology, İstanbul Turkey
melikeusenmez@gmail.com
ORCID ID: 0000-0003-4341-6076

[3]Abdulhamid Han Resarch Hospital Interventional Radiology, İstanbul Turkey
alicanturk.md@gmail.com
ORCID ID: 0000-0001-6145-7029

[4]Selcuk University Faculty of Medicine, Department of Radiology, Konya, Türkiye
ayse.ari@selcuk.edu.tr
ORCID ID: 0000-0001-5778-115X

[5]İstinye University, Faculty of Medicine,
İstanbul, Türkiye
busra.seker1@isu.edu.tr
ORCID ID: 0000-0001-7766-4276

DOI: https://doi.org/10.5281/zenodo.18075401

E mail: ubakyayinevi@gmail.com
www.ubakyayinevi.org
It is responsibility of the author to abide by the publishing ethics rules.
UBAK Publishing House – 2025©

ISBN: 978-625-5753-51-9
December / 2025
Ankara / Turkey

PREFACE

Over the past twenty-five years, medical imaging has progressed far beyond the simple depiction of anatomy, evolving into a central pillar of modern medicine through the integration of artificial intelligence, quantitative assessment, and minimally invasive therapeutic techniques. Among all imaging disciplines, pediatric radiology stands out as one of the most sensitive and demanding fields. The unique radiobiological vulnerability and ongoing developmental processes of children continually reinforce the fundamental principle that pediatric patients are “not merely small adults,” requiring a heightened level of precision and specialized expertise from radiologists.

This book explores pediatric radiology in its full complexity, encompassing a wide spectrum that extends from embryology-based congenital anomalies to advanced digital image analysis and life-saving interventional procedures. The content is structured around five core pillars that reflect contemporary radiological practice:

Fetal and Neonatal Thoracic Radiology: Congenital cystic lung lesions represent conditions in which radiologists play a critical role starting from prenatal diagnosis. This section integrates antenatal ultrasonography and fetal MRI findings with current literature, addressing entities ranging from congenital pulmonary airway malformations to pulmonary sequestration and their implications for postnatal management.

Differential Diagnosis of Abdominopelvic Masses: Cystic abdominal masses in children demonstrate considerable variability in origin and morphology. This chapter highlights characteristic radiological patterns of hepatic, renal, and pelvic lesions, while also presenting practical imaging algorithms that are essential for accurate differential diagnosis.

CT Optimization and Pediatric Emergencies: Ensuring radiation safety in pediatric imaging is both an ethical obligation and a technical challenge. Focusing on emergency conditions such as suspected appendicitis and intussusception, this section discusses contemporary CT protocols and iterative reconstruction techniques designed to achieve optimal diagnostic performance while strictly adhering to the "As Low As Reasonably Achievable" (ALARA) principle.

Quantitative Radiology and Histogram Analysis: Moving beyond subjective visual assessment, modern radiology increasingly relies on quantitative data analysis. Histogram-based approaches enable mathematical modeling of tissue heterogeneity, offering objective insights into tumor characterization and treatment response evaluation.

Therapeutic Radiology (Interventional Approaches): Radiology has expanded its role from diagnosis to treatment. Image guided, minimally invasive interventions now complement and, in some cases, replace surgical procedures in pediatric patients. This section details a wide range of interventional techniques from the management of vascular

anomalies to biopsy procedures emphasizing their technical aspects and clinical impact.

The primary aim of this book is to contribute meaningfully to the rapidly evolving radiological literature and to serve as a reliable reference for daily clinical practice. Through their academically rigorous contributions, the authors not only summarize current knowledge but also provide insight into the future direction of pediatric radiology.

We hope that this work, which bridges scientific depth with clinical applicability, will benefit a broad audience from medical students to experienced specialists. We sincerely thank all contributing authors for their dedication and invaluable efforts.

28/12/2025

EDITOR

Assist. Prof. Dr. Büşra ŞEKER

TABLE OF CONTENTS

CHAPTER 1

IMAGING IN CONGENITAL CYSTIC LUNG LESIONS

Lecturer Dr. Ayşe Arı

1. INTRODUCTION

Congenital cystic lung lesions are pathologies that occur in 1 in 10,000-35,000 births and occur as a series of anomalies(Durell & Lakhoo, 2014). A lung cyst or cystic air space is generally described as a well-defined parenchymal cavity with walls thinner than 2 mm(Odev et al., 2013). Cystic lung lesions may contain air or fluid, or a combination of both, and an air-fluid level is often present(Newman & Caplan, 2014).The etiology of congenital lung lesions is controversial. A widely proposed mechanism is a common embryologic insult that results in airway malformation and airway obstruction. According to this theory, the specific lesion that occurs is determined by the level of airway involvement, the timing of the injury, and the degree of obstruction(Adams et al., 2020). Most of these cystic lesions consist of congenital cystic adenomatoid malformations, pulmonary sequestrations, congenital lobar emphysema, and bronchogenic cysts(Williams & Johnson, 2002). With the widespread use of antenatal ultrasound, the detection of congenital cystic lesions has increased, and the postnatal management process has been facilitated. Additionally, with the increasing use of fetal magnetic rezonans imaging (MRI) , the nature of antenatal cystic lesions can be better determined, and differential diagnosis from extratoracic pathologies has become

relatively easier. Congenital cystic lung lesions may be diagnosed during the antenatal period with symptoms secondary to the lesion or during routine screening, or they may be diagnosed incidentally during childhood.

2. ANTENATAL IMAGING IN CONGENITAL PULMONARY CYSTIC LESIONS - ULTRASOUND AND MRI

Congenital lung lesions are a rare group of developmental lung anomalies and are usually first detected prenatally during routine second-trimester ultrasound examination. Various findings are observed in the fetus. Some lesions, when large, exert a significant mass effect on adjacent structures in the chest cavity. Masses occupying space in the chest can cause pulmonary hypoplasia by preventing normal lung growth. Mass effect on the mediastinum may cause impaired venous return and fetal hydrops. Compression of the esophagus may disrupt normal fetal swallowing and lead to polyhydramnios. These findings may require intrauterine or perinatal intervention.High-resolution ultrasound performed during the second trimester is the primary imaging method for antenatal detection of congenital lung lesions. Color Doppler ultrasound is important in evaluating pulmonary vascular structure to help differentiate between various malformations. Complementary imaging with fetal magnetic resonance imaging (MRI) may be helpful in better defining lesions and adjacent structures, particularly the trachea and contralateral lung(Sintim-Damoa & Cohen, 2022).

The lungs are homogeneous in terms of echogenicity on ultrasound and hypoechoic relative to the liver in early pregnancy.The diaphragm appears as a thin, curved structure between the lungs and the upper abdomen. It is hypoechoic compared to both the lungs and the liver. The ribs are highly echogenic, curved structures originating from the spine and extending forward around the circumference of the chest. In T2-weighted MRI imaging, fetal lungs appear homogeneously hyperintense. Lung maturation leads to an increase in the number of alveoli and, consequently, an increase in alveolar fluid production. As a result, signal intensity in T2-weighted images increases after the 24th week of pregnancy(Adams et al., 2020).

When a lesion is observed in the lung, prenatal diagnosis should be made by determining which subtype it is based on an evaluation of the lesion's vascular supply, appearance, size, and the presence of hydrops fetalis. Congenital lung cystic disease (CLCD) is characterized by cyst formation or increased echogenicity in the fetal chest(Miyazaki, 2020).The classification of CLCD is based on the pathological findings of the lesion, taking into account the primary formation during lung development. The classification is as follows: (1) pulmonary airway malformation such as congenital pulmonary airway malformation (CPAM), (2) lung bud malformation such as bronchopulmonary sequestration (BPS), (3) foregut malformation such as bronchogenic cyst, (4) bronchial atresia, and (5) others.The first step is to determine the source of blood supply to the lung lesion. The majority of CLCD lesions are supplied by the pulmonary circulation. However, BPS, which is categorised as a pulmonary bud malformation, is supplied by

the systemic circulation. BPS is a solid, hyperechoic lung mass with systemic feeding vessels(Figure 1). It is seen as a mass of nonfunctional lung tissue that is not connected to the bronchial tree(Hernanz-Schulman et al., 1991). If systemic blood supply is absent, the second step is for the appearance of the CLCD lesion to be evaluated. The majority of such lesions are classified as CPAM or bronchial atresia with communication with the bronchial tree. The appearance ranges from homogeneous, without a typical cyst, to a multiple-cystic appearance. Stocker's classification of pathological findings uses the following three categories for cyst size: >1 cm, 0.5–1 cm, and <0.5 cm (Stocker et al., 1977).Adzick et al. classified lesions into two categories based on the gross appearance on ultrasound(Adzick et al., 1985). Macrocystic lesions are defined as single or multiple cysts with a diameter of ≥0.5 cm. In contrast, microcystic lesions are characterised as solid or dense cysts with a diameter of <0.5 cm.

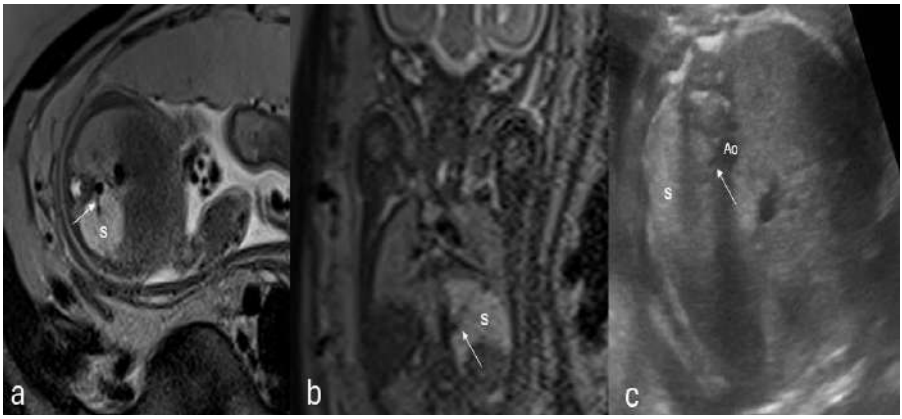

Figure 1. Bronchopulmonary sequestration. Axial(a) and coronal(b) T2-weighted MRI at 22 weeks of gestation shows a hyperintense left

thoracic mass(S) extending up to the diaphragm. A tubular hypointense supplying vessel (arrow) arises from the descending thoracic aorta.Transverse sonographic image(c) at in the same fetus 22 weeks of gestation shows a hyperechoic mass (S) at the posterior left lung base. The tubular hypoechoic feeding vessel (arrow) emerges from the descending thoracic aorta(Ao).

3. CONGENITAL LUNG PATHOLOGY

3.1. Congenital pulmonary airway malformation

Congenital pulmonary airway malformations are defined by areas of over-proliferation and dilatation of terminal respiratory bronchioles, with an absence of normal alveoli. CPAMs are intrapulmonary lesions that contain various types of epithelial lining and maintain communication with the normal trachea-bronchial tree, as well as retaining a normal blood supply(Adams et al., 2020).

Stocker and colleagues pathologically classified CPAM into three types based on cyst size and histological similarity to segments of the developing bronchial tree and air spaces. According to the Stocker classification, type I CPAMs consist of one or more large cysts, the largest of which is 2-10 cm in diameter.Type I CPAMs are the most common type of CPAM and are often seen at birth with respiratory distress. Stocker type II CPAMs consist of multiple small cysts measuring 0.5-2 cm in size.Type II CPAMs are generally associated with other congenital anomalies. Type III CPAMs have small cysts measuring less than 0.5 cm and typically appear completely solid on ultrasound(Stocker et al., 1977).

CPAMs are generally detected incidentally during the prenatal period. Sonographically, CPAMs may appear anechoic, containing multiple cysts of varying sizes with echogenic lung parenchyma; or they may appear primarily hyperechoic and solid, with scattered cysts or without cysts. In type III CPAM, tiny cysts that are too small to be visualized on US cause the CPAM to appear echogenic by providing multiple interfaces that reflect sound waves to each other. Color Doppler may show vascular flow from pulmonary artery branches. Fetal MRI also typically shows cystic, solid, or mixed cystic and solid masses that are hyperintense relative to normal lung parenchyma on T2-weighted imaging(Figure 2). Focal cystic components in mixed cystic and solid CPAMs usually have higher signal intensity than the surrounding solid components(Sintim-Damoa & Cohen, 2022).

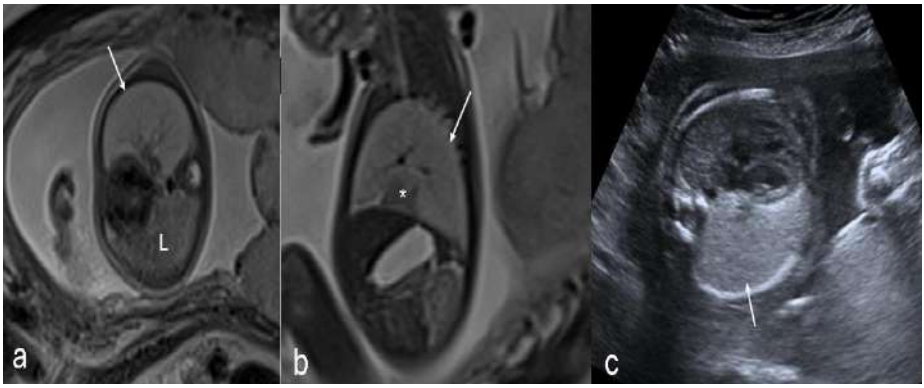

Figure 2. Congenital pulmonary airway malformation, type 3. Axial T2-weighted MRI at 24 weeks of gestation (a) demonstrates a predominantly hyperintense mass lesion (arrow) occupying nearly the entire left hemithorax with mild rightward cardiac displacement. The normal right lung (L) on the contralateral side shows comparatively lower signal intensity. Sagittal T2-weighted MRI (b) shows the lesion

(indicated by the arrow) and a small region of normal lung parenchyma preserved above the diaphragm (indicated by the asterisk). Transverse ultrasound imaging (c) shows a hyperechoic mass filling the left hemithorax(arrow).

Patients with CPAM typically present with symptoms such as respiratory distress and recurrent infections during the neonatal or infant period. However, CPAM can also be detected incidentally in asymptomatic elderly children. Chest radiography and low-dose computed tomography (CT) angiography can be used to evaluate CPAMs in postnatal imaging. Chest radiographs may be normal; alternatively, they may show mediastinal shifted or non-shifted cystic or solid masses(Figure 3).

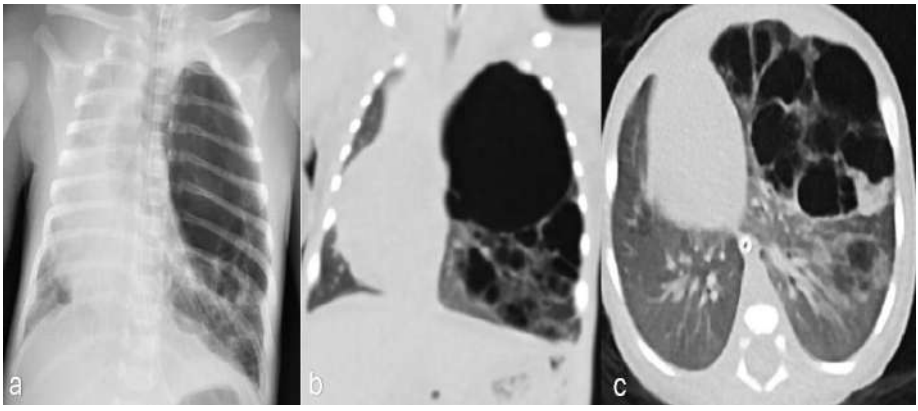

Figure 3. Newborn presenting with a prenatally diagnosed type 1 CPAM. (a) Chest radiograph shows multiple air-filled cysts with septa occupying the entire left hemithorax, with mediastinal shift to the contralateral side. Coronal (b) and axial (c) CT scan (lung window) shows air-filled, thin-walled spaces of varying size.

Type I CPAMs sometimes appear as masses with large air-filled cystic structures on CT imaging(Figure 4). Type II CPAMs appear as air-filled mixed cystic and solid masses, while type III CPAMs appear as solid masses.

Figure 4. Congenital pulmonary airway malformation type 1 in a 10-month-old infant. Chest radiograph(a) shows an area of hyperlucency (arrow) in the right lower lobe. Axial(b) and sagittal(c) CT images in the lung parenchyma window demonstrate a lobulated, air-filled cyst in the right lower lobe containing multiple thin internal septa and appearing uniloculated(arrow) with surrounding areas compatible with air trapping(asteriks).

CPAMs complicated by infection may have thick contrast-enhancing walls and may contain air-fluid levels(Figure 5). In elderly patients with recurrent pneumonia, it may be difficult to distinguish whether the visualized lung cysts are due to recurrent infection and pneumothorax formation or an underlying congenital cystic lung lesion .CT angiography of CPAMs shows arterial blood flow from the pulmonary

artery, as normally expected. The absence of a feeding vessel in the aorta helps differentiate CPAM from bronchopulmonary sequestration and hybrid lesions(Lee et al., 2008).

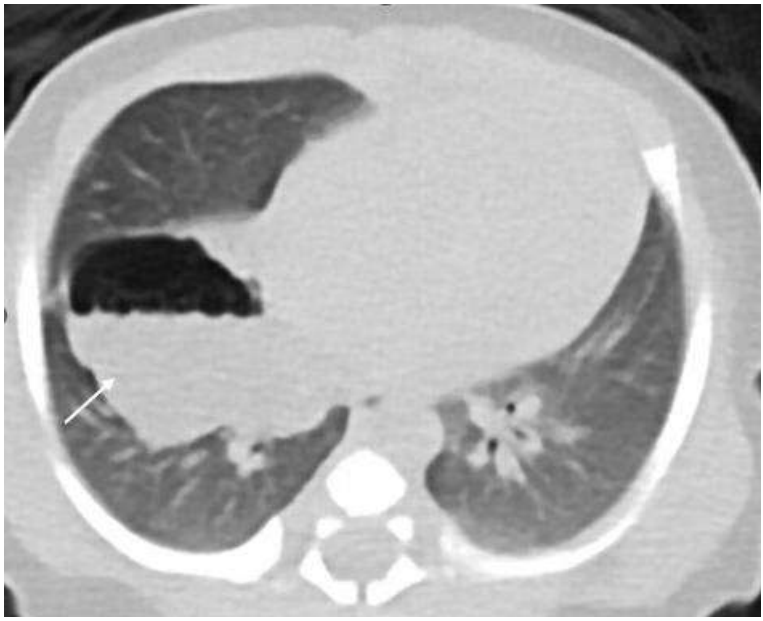

Figure 5. A complex CPAM lesion showing air-fluid levels on axial CT scan in a patient with CPAM type 1.

3.2. Bronchopulmonary sequestration

Bronchopulmonary sequestration is abnormal, non-functional lung tissue that is not connected to the tracheobronchial tree. Its blood supply comes from systemic vessels. There are two types of pulmonary sequestration: extralobar sequestration(ELS) (25%) and intralobar sequestration(ILS). Abnormal lung tissue is located in the visceral pleura of pulmonary lobes in the intralobar type, while in the extralobar type, it has its own visceral pleura. Extralobar venous drainage typically occurs in systemic veins, whereas intralobar drainage occurs in

pulmonary veins. ILSs are most commonly found in the lower lobes, slightly more frequently on the left side, and more frequently in the posterior basal segment. ELSs are most commonly located in the left posterior costodiaphragmatic sulcus between the lower lobe and the left hemidiaphragm.Extralobar sequestrations may be supradiaphragmatic, subdiaphragmatic, or intradiaphragmatic(Abbey et al., 2009; Bulas & Egloff, 2011).

On fetal ultrasound, ELS typically appears as a solid, well-defined, triangular, echogenic mass lesion. Color Doppler can detect a feeding vessel originating from the aorta. If sequestration is located below the diaphragm, it may appear as an echogenic intra-abdominal mass resembling a suprarenal mass such as neuroblastoma(Kalenahalli et al., 2013). Fetal MRI is supportive in confirming the diagnosis of BPS and can also be used to estimate the volume and maturity of normal lung tissue.Another advantage of fetal MRI is the evaluation of other associated diseases, such as CPAM (a hybrid lesion) and congenital diaphragmatic hernias, which are common in the extralobar type(Miyazaki, 2020).

The most common radiographic finding in patients with sequestration is a focal lung mass, located within the bilateral lower lobes (98%), with the left side more frequently involved than the right side. CT angiography can help determine the location of bronchopulmonary sequestration and systemic arterial supply and identify venous drainage.Imaging should be performed from the thoracic inlet to just above the renal arteries to ensure that subdiaphragmatic sequestrations

and systemic feeders originating from the abdominal aorta are visualized (Figure 6) (Lee et al., 2008).

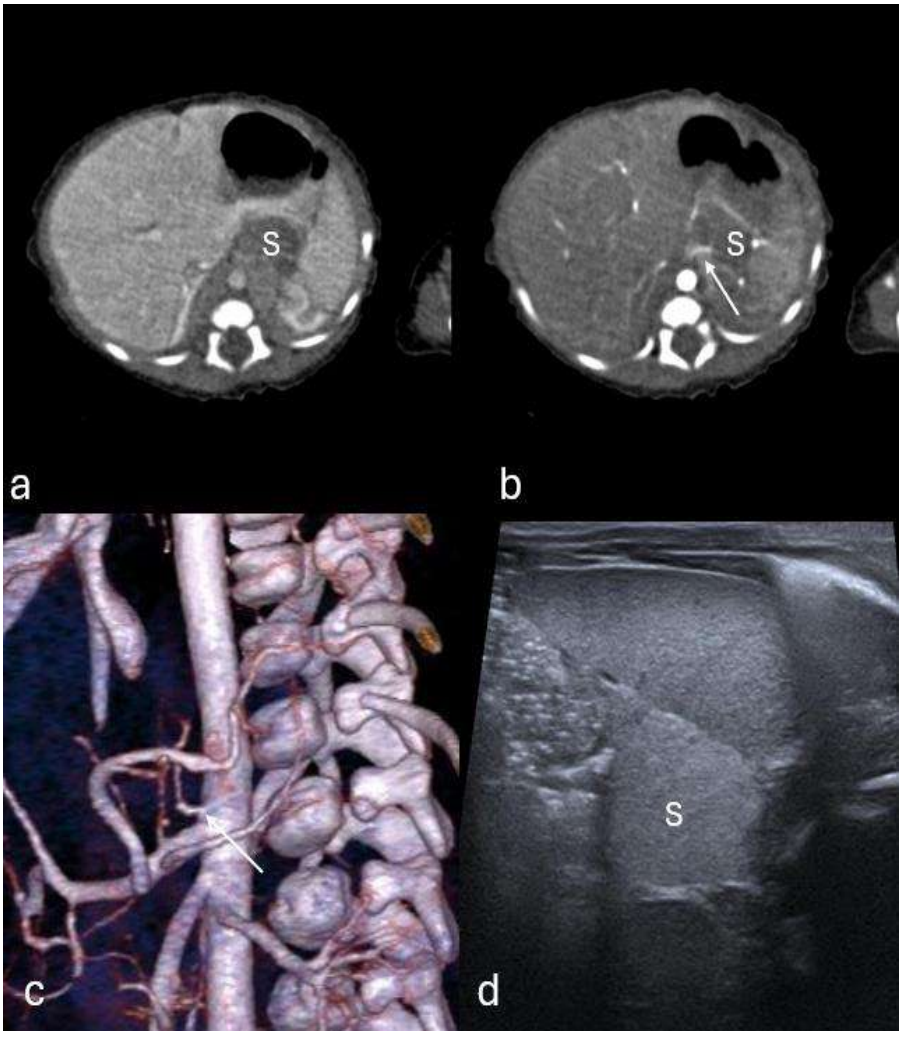

Figure 6. Extralobar bronchopulmonary sequestration. Axial portal venous and arterial phase CT images of the abdomen (a, b) demonstrate a mass lesion in the mid to left upper quadrant, adjacent to the adrenal gland and spleen, consistent with sequestration, with a feeding artery

originating from the abdominal aorta (arrow), while the VRT image (c) delineates the feeding artery(arrow) and ultrasound shows a hyperechoic mass lesion adjacent to the spleen (S).

3.3. Congenital lobar emphysema

Congenital lobar emphysema is defined as hyperinflation in one or more lung lobes, causing compression of surrounding structures. This compression may lead to mediastinal shift. The left upper or right middle lobes are most commonly affected. The etiology of congenital lobar emphysema (CLE) is idiopathic in about half of cases. In the remainder, air trapping results from intrinsic or extrinsic factors. Intrinsic causes include deficient bronchial cartilage, mucosal proliferation, mucus plugging, bronchial torsion, or atresia. Extrinsic causes involve external compression of the bronchi by vessels, lymph nodes, cysts, or focal pulmonary hypoplasia(Durell & Lakhoo, 2014).

Prenatal US shows a homogeneous hyperechoic mass. Mediastinal shift and herniation of the affected lung to the contralateral side might be seen. On fetal MRI, it appears as a homogeneous hyperintense mass with lobar distribution (Bulas & Egloff, 2011).

Chest X-rays may initially show focal opacity of retained fetal lung fluid.Over time, the affected lobe appears hyperlucent. A mass effect may be seen with mediastinal shift from the affected lobe. CT confirms the radiographic findings, showing hyperinflation and hyperlucency of the CLE and decreased vascularity. Mediastinal shift to the contralateral hemithorax is also frequently seen(Lee et al., 2011).

3.4. Bronchogenic cyst

Congenital bronchogenic cysts form as a result of abnormal budding from the ventral embryonic foregut along the tracheobronchial tree, and this budding subsequently typically transforms into a fluid-filled, blind-ended sac located in the mediastinum near the tracheal carina. Less commonly, cysts may also form in the lung parenchyma, pleura, or diaphragm. Bronchogenic cyst walls are thin, lined with respiratory epithelium, and contain mucous material(Liu et al., 2013).

In prenatal US, bronchogenic cysts are generally round, single-lumen, and anechoic, but layered echogenic remnants may be seen.There is no internal color Doppler flow. Bronchogenic cysts are T2 hyperintense on fetal MRI(Bulas & Egloff, 2011).

Chest radiographs typically show a well-defined, rounded subcarinal opacity. Chest CT shows a fluid-filled mass, but the internal contents have a higher attenuation capability if proteinaceous or hemorrhagic content is present. Uncomplicated bronchogenic cysts do not show internal contrast enhancement. Infected bronchogenic cysts may show a thick rim of enhancement or air-fluid levels on CT(Coley, 2018).

3.5. Bronchial atresia

Bronchial atresia results from local obliteration or stenosis at or near the origin of the segmental, subsegmental, or lobar bronchus.Bronchial atresia causes homogeneously increased echogenicity on antenatal ultrasound and high signal intensity on T2-weighted fetal MRI images of the affected lung(Miyazaki, 2020).

Radiographic features include hilar mass and peripheral lung hyperinflation; this is usually associated with an opaque round mucocele in the bronchial tree immediately distal to the obstruction(Zylak et al., 2002). In CT, congenital bronchial atresia typically appears as a central, tubular, or nodular opacity that may show an air-fluid level reflecting a mucus-filled, dilated bronchus. It most commonly involves the apical or apicoposterior segment of the upper lobes. Adjacent lung hyperinflation due to collateral ventilation and decreased vascular markings in the affected area are characteristic. CT provides the most accurate assessment by clearly demonstrating mucus impaction, segmental hypoattenuation, and decreased vascularity(Lee et al., 2008).

3.6. Pleuropulmonary blastoma

Pleuropulmonary blastoma (PPB) is the most frequent primary lung malignancy in children, usually occurring within the first seven years of life. It is classified into three types: type I (predominantly cystic), type II (mixed cystic and solid), and type III (solid). Type I PPB, often detected in infancy, can closely resemble other congenital cystic lung lesions such as CPAM, making differentiation challenging. Although type I has the best prognosis, it may progress to the more aggressive type II or III forms, highlighting the importance of early recognition and management(Messinger et al., 2015).

On imaging, cystic and mixed-type PPB typically appear as thin-walled, air-filled cysts, but may contain fluid in the prenatal or early neonatal period. When infected, cysts may become thick-walled or

show air-fluid levels. They may be single-chambered or multi-chambered, ranging from small lesions to large cysts covering the entire hemithorax. Systemic feeding vessels are absent. Spontaneous pneumothorax occurs in approximately 30% of cystic PPB cases, and the disease may be bilateral or multifocal (Guillerman et al., 2019).

3.7. Congenital high-airway obstruction syndrome

Congenital high airway obstruction syndrome (CHAOS) is a series of conditions that begin with complete or near-complete obstruction of the fetal high airway. Obstruction of the fetal airway prevents normal drainage of lung fluid, causing its accumulation and leading to pulmonary hyperplasia and overexpansion. The enlarged, fluid-filled lungs compress the mediastinum, obstruct venous return, and can subsequently result in ascites and hydrops fetalis.Prenatal imaging shows bilateral, symmetrically enlarged lungs that appear hyperechoic on US. CHAOS shows characteristic prenatal MRI features, including markedly enlarged, hyperintense lungs, flattened or inverted diaphragms, and a dilated airway distal to the obstruction. Additional findings often include massive ascites, a centrally displaced and compressed heart, and placentomegaly(Guimaraes et al., 2009; Leal et al., 2018). Survival in CHAOS can be achieved using an ex utero intrapartum treatment (EXIT) procedure, where the fetus is partially delivered to secure a functional airway while still receiving oxygen through the placental circulation(Sintim-Damoa & Cohen, 2022).

4. SUMMARY OF IMPORTANT IMAGING FEATURES

Differentiating congenital lung lesions can be challenging due to overlapping imaging features. CPAM, bronchopulmonary sequestration, congenital lobar overinflation, and bronchial atresia may all appear hyperechoic on fetal ultrasound and hyperintense on T2-weighted MRI, and hybrid lesions are common. When a definitive diagnosis is not possible, lesion size, location, and imaging characteristics—including mass effect, mediastinal shift, diaphragm shape, and lung volume—should be reported. Decreased echogenicity on ultrasound or signal loss on MRI suggests pulmonary hypoplasia(Adams et al., 2020).

Features useful for differentiating congenital lung anomalies include the detection of a systemic feeding artery and the presence of cysts within the lesion, making detailed vascular analysis essential. The identification of a systemic feeding vessel supports a diagnosis of bronchopulmonary sequestration or a hybrid lesion. Careful assessment of venous drainage can further classify a sequestration as intralobar or extralobar, as intralobar sequestrations drain into the pulmonary veins while extralobar sequestrations drain into systemic veins. Bronchogenic cysts typically present as single, unilocular cystic masses, often located in the subcarinal region, whereas centrally located round or tubular cystic structures may represent a bronchocele or mucocele. When these findings are associated with a hyperechoic or hyperintense lung mass, bronchial atresia should be considered. Thorough evaluation of both prenatal and postnatal images is crucial, as the presence of bronchial atresia is frequently associated with hybrid lesions and may support

conservative management in asymptomatic infants, particularly when the lesion is small. Multiple cysts are a common feature in several lung malformations, such as CPAM or hybrid lesions(Sintim-Damoa & Cohen, 2022)

5. CONCLUSION

Congenital lung lesions are a diverse group of malformations that can present with a variety of clinical symptoms. Although a definitive diagnosis often requires pathological confirmation, prenatal ultrasound and MRI scans are crucial for characterising the lesions, predicting outcomes and guiding perinatal management. Postnatal imaging, including CT angiography of the chest and upper abdomen, provides further information about these lesions, which are often identified antenatally, and supports treatment planning, including consideration of surgical resection.

6. REFERENCES

Abbey, P., Das, C., Pangtey, G., Seith, A., Dutta, R., & Kumar, A. (2009). Imaging in bronchopulmonary sequestration. *Journal of Medical Imaging and Radiation Oncology*, *53*(1), 22-31.

Adams, N. C., Victoria, T., Oliver, E. R., Moldenhauer, J. S., Adzick, N. S., & Colleran, G. C. (2020). Fetal ultrasound and magnetic resonance imaging: a primer on how to interpret prenatal lung lesions. *Pediatric Radiology*, *50*(13), 1839-1854.

Adzick, N. S., Harrison, M. R., Glick, P. L., Golbus, M. S., Anderson, R. L., Mahony, B. S., Callen, P. W., Hirsch, J. H., Luthy, D. A., & Filly, R. A. (1985). Fetal cystic adenomatoid malformation: prenatal diagnosis and natural history. *Journal of pediatric surgery*, *20*(5), 483-488.

Bulas, D., & Egloff, A. M. (2011). Fetal chest ultrasound and magnetic resonance imaging: recent advances and current clinical applications. *Radiol Clin North Am*, *49*(5), 805-823. https://doi.org/10.1016/j.rcl.2011.06.005

Coley, B. D. (2018). *Caffey's Pediatric Diagnostic Imaging E-Book: Caffey's Pediatric Diagnostic Imaging E-Book*. Elsevier Health Sciences.

Durell, J., & Lakhoo, K. (2014). Congenital cystic lesions of the lung. *Early Hum Dev*, *90*(12), 935-939. https://doi.org/10.1016/j.earlhumdev.2014.09.014

Guillerman, R. P., Foulkes, W. D., & Priest, J. R. (2019). Imaging of DICER1 syndrome. *Pediatric Radiology*, *49*(11), 1488-1505.

Guimaraes, C. V., Linam, L. E., Kline-Fath, B. M., Donnelly, L. F., Calvo-Garcia, M. A., Rubio, E. I., Livingston, J. C., Hopkin, R. J., Peach, E., Lim, F. Y., & Crombleholme, T. M. (2009). Prenatal MRI findings of fetuses with congenital high airway obstruction sequence. *Korean J Radiol*, *10*(2), 129-134. https://doi.org/10.3348/kjr.2009.10.2.129

Hernanz-Schulman, M., Stein, S., Neblett, W., Atkinson, J., Kirchner, S., Heller, R., Merrill, W., & Fleischer, A. (1991). Pulmonary sequestration: diagnosis with color Doppler sonography and a new theory of associated hydrothorax. *Radiology*, *180*(3), 817-821.

Kalenahalli, K. V., Garg, N., Goolahally, L. N., Reddy, S. P., & Iyengar, J. (2013). Infradiaphragmatic extralobar pulmonary sequestration: masquerading as suprarenal mass. *Journal of Clinical Neonatology*, *2*(3), 146-148.

Leal, V. L. L., Cortés, L. M., & Del Del Cacho, C. S. (2018). Prenatal diagnosis of congenital high airway obstruction syndrome. *Indian Journal of Radiology and Imaging*, *28*(03), 366-368.

Lee, E. Y., Boiselle, P. M., & Cleveland, R. H. (2008). Multidetector CT evaluation of congenital lung anomalies. *Radiology*, *247*(3), 632-648.

Lee, E. Y., Dorkin, H., & Vargas, S. O. (2011). Congenital pulmonary malformations in pediatric patients: review and update on etiology, classification, and imaging findings. *Radiologic Clinics*, *49*(5), 921-948.

Liu, Y.-P., Lin, Y.-L., & Chen, S.-C. (2013). Fetal magnetic resonance imaging of congenital chest malformations: a pictorial review. *Journal of Radiological Science*, *38*(4), 119-127.

Messinger, Y. H., Stewart, D. R., Priest, J. R., Williams, G. M., Harris, A. K., Schultz, K. A., Yang, J., Doros, L., Rosenberg, P. S., Hill, D. A., & Dehner, L. P. (2015). Pleuropulmonary blastoma: a report on 350 central pathology-confirmed pleuropulmonary blastoma cases by the International Pleuropulmonary Blastoma Registry. *Cancer*, *121*(2), 276-285. https://doi.org/10.1002/cncr.29032

Miyazaki, O. (2020). Fetal Diagnostic Imaging of Congenital Cystic Lung Disease. In H. Sago, H. Okuyama, & Y. Kanamori (Eds.), *Congenital Cystic Lung Disease: Comprehensive Understanding of its Diagnosis and Treatment from Fetus to Childhood* (pp. 27-37). Springer Singapore. https://doi.org/10.1007/978-981-15-5175-8_4

Newman, B., & Caplan, J. (2014). Cystic Lung Lesions in Newborns and Young Children: Differential Considerations and Imaging. *Seminars in Ultrasound, CT and MRI*, *35*(6), 571-587. https://doi.org/https://doi.org/10.1053/j.sult.2014.07.001

Odev, K., Guler, İ., Altinok, T., Pekcan, S., Batur, A., & Ozbiner, H. (2013). Cystic and cavitary lung lesions in children: radiologic findings with pathologic correlation. *Journal of clinical imaging science*, *3*, 60.

Sintim-Damoa, A., & Cohen, H. L. (2022). Fetal imaging of congenital lung lesions with postnatal correlation. *Pediatric Radiology*, *52*(10), 1921-1934. https://doi.org/10.1007/s00247-022-05465-w

Stocker, J. T., Madewell, J. E., & Drake, R. M. (1977). Congenital cystic adenomatoid malformation of the lung: classification and morphologic spectrum. *Human pathology*, *8*(2), 155-171.

Williams, H. J., & Johnson, K. J. (2002). Imaging of congenital cystic lung lesions. *Paediatr Respir Rev*, *3*(2), 120-127.

Zylak, C. J., Eyler, W. R., Spizarny, D. L., & Stone, C. H. (2002). Developmental lung anomalies in the adult: radiologic-pathologic correlation. *Radiographics*, *22*(suppl_1), S25-S43.

CHAPTER 2

HISTOGRAM ANALYSIS IN RADIOLOGICAL DIAGNOSIS

Specialist Dr. Hasan Genç

INTRODUCTION

Advancements in radiological imaging technologies have facilitated the transition from traditional visual assessments to routine quantitative analyses. Throughout this development, histogram analysis has emerged as a significant method that mathematically evaluates the intensity distribution of tissue pixels and provides diagnostic value (Huff et al., 2021).

Histogram analysis objectively assesses tissue heterogeneity in radiological modalities such as magnetic resonance imaging (MRI), computed tomography (CT), positron emission tomography (PET), and mammography (Kim et al., 2023). By revealing microstructural variations that may be overlooked during manual interpretation, this method enhances diagnostic accuracy.

FUNDAMENTAL PRINCIPLES OF HISTOGRAM ANALYSIS

A histogram is a statistical graph that represents the frequency distribution of intensity values of all pixels within an image. The x-axis denotes the gray-level values, while the y-axis indicates the number of pixels corresponding to each value. Mathematically, the histogram

function $H(i)$defines the frequency of pixels with a specific intensity level as follows:

$$H(i) = \sum_{x=1}^{M} \sum_{y=1}^{N} \delta(f(x,y) - i)$$

Here, $f(x,y)$represents the pixel intensity value, and δdenotes the Kronecker delta function (Sporring & Darkner, 2022).

In histogram analysis, statistical parameters such as mean, standard deviation, skewness, and kurtosis are commonly evaluated. The mean value reflects tissue brightness, the standard deviation indicates homogeneity, and skewness and kurtosis characterize the symmetry and sharpness of the distribution, respectively (Huang et al., 2023).

In recent years, histogram analysis has been effectively integrated with artificial intelligence and machine learning algorithms, playing a significant role in automated image classification processes (Wang et al., 2023).

HISTOGRAM CHARACTERISTICS IN RADIOLOGICAL IMAGING

Histogram profiles in radiological images vary depending on the contrast mechanism of the imaging modality:

- **CT Images:**

  The histogram is defined based on Hounsfield units (HU). Different tissues such as soft tissue, air, and bone create distinct peaks due to their specific intensity ranges. In low-dose CT systems, histogram-based noise correction algorithms have been successfully implemented (Lee & Goo, 2018).

- **MR Images:**

  Histogram profiles depend on tissue proton density and relaxation times. The histograms of T1- and T2-weighted images differ significantly, and these differences carry diagnostic value, particularly in tumor grading (Li et al., 2021).

- **PET Images:**

  The histogram reflects the distribution of the Standardized Uptake Value (SUV). High-entropy histograms are generally indicative of malignant lesions (Amrane et al., 2023).

Histogram analysis is also frequently employed in region-of-interest (ROI)–based radiomic modeling (van Timmeren et al., 2020).

THE CONTRIBUTION OF HISTOGRAM ANALYSIS IN CLINICAL PRACTICE

1. **Oncologic Imaging**

   Histological heterogeneity within tumor tissues is directly associated with the degree of malignancy. Histogram analysis provides objective quantification of this heterogeneity, thereby contributing to diagnostic and staging processes. MRI histogram parameters have demonstrated high accuracy in grading gliomas and breast cancers (Gihr et al., 2022).

2. **Liver Diseases**

   CT-based histogram analysis serves as a noninvasive tool for evaluating hepatic steatosis and fibrosis. Histogram parameters have been reported to show strong correlation with magnetic resonance elastography (MRE) findings (Xu et al., 2021).

3. **Pulmonary and Cardiac Imaging**

   CT histogram analysis quantitatively determines the extent of diseases such as emphysema and fibrosis within the lung parenchyma. Cardiac MRI histogram parameters are valuable in assessing the extent of myocardial fibrosis (Di Renzi et al., 2021).

4. **Neurological Disorders**

   Diffusion tensor imaging (DTI) histogram analysis can reveal

microstructural deterioration of white matter in neurodegenerative diseases such as Alzheimer's disease, Parkinson's disease, and Multiple Sclerosis. Alterations in Fractional Anisotropy (FA) and Mean Diffusivity (MD) histograms indicate early neurodegeneration (Takahashi et al., 2024).

ADVANTAGES, LIMITATIONS, AND FUTURE PERSPECTIVES

Histogram analysis is an objective, reproducible, and quantitative method in radiological diagnosis. However, it has several limitations:

- Variations in imaging parameters may influence histogram outcomes.
- ROI selection remains operator-dependent.
- Histogram analysis includes only first-order statistics and does not assess spatial relationships.

To overcome these limitations, histogram analysis is increasingly being integrated with texture analysis, radiomic feature extraction, and AI-based models (Baeßler et al., 2024). In the future, the integration of histogram-based radiomic features with genetic data is expected to strengthen personalized diagnostic and therapeutic strategies (Li et al., 2022).

CONCLUSION

Histogram analysis provides significant contributions to the diagnostic process by quantitatively evaluating information derived from radiological images. Due to its ease of application, low cost, and high reproducibility, it is widely utilized in both clinical practice and research settings. The integration of histogram analysis with artificial intelligence–based systems is expected to make it an indispensable component of radiological diagnosis in the future.

REFERENCES

Amrane, K., Thuillier, P., Bourhis, D., Le Meur, C., Quere, C., Leclere, J.-C., Ferec, M., Jestin-Le Tallec, V., Doucet, L., Alemany, P., Salaun, P.-Y., Metges, J.-P., Schick, U., & Abgral, R. (2023). Prognostic value of pre-therapeutic FDG-PET radiomic analysis in gastro-esophageal junction cancer. Scientific Reports, 13, 5789. https://doi.org/10.1038/s41598-023-31587-8

Baeßler, B., Engelhardt, S., Hekalo, A., Hennemuth, A., Hüllebrand, M., Laube, A., Scherer, C., Tölle, M., & Wech, T. (2024). Perfect match: Radiomics and artificial intelligence in cardiac imaging. Circulation: Cardiovascular Imaging, 17(6). https://doi.org/10.1161/CIRCIMAGING.123.015490

Di Renzi, P., Coniglio, A., Abella, A., Belligotti, E., Rossi, P., Pasqualetti, P., Simonelli, I., & Della Longa, G. (2021). Volumetric histogram-based analysis of cardiac magnetic resonance T1 mapping: A tool to evaluate myocardial diffuse fibrosis. Physica Medica, 82, 185–191. https://doi.org/10.1016/j.ejmp.2021.01.080

Gihr, G., Horvath-Rizea, D., Kohlhof-Meinecke, P., Ganslandt, O., Henkes, H., Härtig, W., Donitza, A., Skalej, M., & Schob, S. (2022). Diffusion weighted imaging in gliomas: A histogram-based approach for tumor characterization. Cancers, 14(14), 3393. https://doi.org/10.3390/cancers14143393

Huang, C., Zhan, C., Hu, Y., Yin, T., Grimm, R., & Ai, T. (2023). Histogram analysis of breast diffusion kurtosis imaging: A

comparison between readout-segmented and single-shot echo-planar imaging sequence. Quantitative Imaging in Medicine and Surgery, 13(2), 735–746. https://doi.org/10.21037/qims-22-475

Huff, D. T., Ferjancic, P., Namías, M., Emamekhoo, H., Perlman, S. B., & Jeraj, R. (2021). Image intensity histograms as imaging biomarkers: Application to immune-related colitis. Biomedical Physics & Engineering Express, 7(6), 10.1088/2057-1976/ac27c3. https://doi.org/10.1088/2057-1976/ac27c3

Kim, H.-Y., Bae, M.-S., Seo, B.-K., Lee, J.-Y., Cho, K.-R., Woo, O.-H., Song, S.-E., & Cha, J. (2023). Comparison of CT- and MRI-based quantification of tumor heterogeneity and vascularity for correlations with prognostic biomarkers and survival outcomes: A single-center prospective cohort study. Diagnostics, 13(7), 1205. https://doi.org/10.3390/diagnostics13071205

Lee, K. B., & Goo, H. W. (2018). Quantitative image quality and histogram-based evaluations of an iterative reconstruction algorithm at low-to-ultralow radiation dose levels: A phantom study in chest CT. Korean Journal of Radiology, 19(1), 119–129. https://doi.org/10.3348/kjr.2018.19.1.119

Li, Q., Xiao, Q., Yang, M., Chai, Q., Huang, Y., Wu, P.-Y., Niu, Q., & Gu, Y. (2021). Histogram analysis of quantitative parameters from synthetic MRI: Correlations with prognostic factors and molecular subtypes in invasive ductal breast cancer. European Journal of Radiology, 139, 109697. https://doi.org/10.1016/j.ejrad.2021.109697

Li, S., Wu, J., Zhang, J., Sun, X., & Zhang, Y. (2022). Radiomics and genomics in precision medicine: A review of applications in oncology. Frontiers in Oncology, 12, 980158. https://doi.org/10.3389/fonc.2022.980158

Sporring, J., & Darkner, S. (2022). Reconstructing binary signals from local histograms. Entropy, 24(1), 37. https://doi.org/10.3390/e24010037

Takahashi, H., Takami, Y., Takeda, S., Hayakawa, N., Nakajima, T., Takeya, Y., Matsuo-Hagiyama, C., Arisawa, A., Rakugi, H., & Tomiyama, N. (2024). Imaging biomarker for early-stage Alzheimer disease: Utility of hippocampal histogram analysis of diffusion metrics. American Journal of Neuroradiology, 45(3), 320–327. https://doi.org/10.3174/ajnr.A8106

van Timmeren, J. E., Cester, D., Tanadini-Lang, S., Alkadhi, H., & Baessler, B. (2020). Radiomics in medical imaging—"how-to" guide and critical reflection. Insights into Imaging, 11, 91. https://doi.org/10.1186/s13244-020-00887-2

Wang, H., Xu, X., Zhang, W., Guo, Y., & Jin, Q. (2023). Radiomics and its feature selection: A review. Symmetry, 15(10), 1834. https://doi.org/10.3390/sym15101834

Xu, X., Zhu, H., Li, R., Lin, H., Grimm, R., Fu, C., & Yan, F. (2021). Whole-liver histogram and texture analysis on T1 maps improves the risk stratification of advanced fibrosis in NAFLD. European Radiology, 31, 1748–1759. https://doi.org/10.1007/s00330-020-07235-4

CHAPTER 3

COMPUTED TOMOGRAPHY IN PEDIATRIC ACUTE ABDOMEN DIAGNOSTIC APPROACH, SYSTEMATIC DIFFERENTIAL DIAGNOSIS, AND RADIATION DOSE OPTIMIZATION

Specialist Dr. Melike Yeşildal

1. INTRODUCTION

1.1. Overview: Pediatric Acute Abdomen and Diagnostic Challenges

While **acute abdomen** in the pediatric population constitutes a significant proportion of Emergency Department presentations, the diagnostic approach differs notably from that of adults. Pediatric patients may have limited ability to localize and articulate their symptoms. This frequently leads to diagnostic uncertainty, particularly in younger age groups and in cases presenting with atypical conditions (e.g., perforated appendicitis).

Within a broad spectrum of differential diagnoses (including gastrointestinal, genitourinary, gynecological, pulmonary, and vascular etiologies), the rapid and accurate differentiation of surgical emergencies is of critical importance. Delays in the diagnostic process increase morbidity, while unnecessary surgical interventions can also have long-term negative effects on patient health. Therefore, accurate and prompt diagnosis is a primary responsibility of the radiologist.

1.2. Role and Limitations of CT

The imaging algorithm is shaped by the axes of diagnostic certainty and patient safety (1).
When pediatric acute abdomen is suspected, the generally accepted approach is that modalities not utilizing ionizing radiation should be the first-line choice.

- Ultrasonography (USG): This is the primary imaging modality as it offers high diagnostic sufficiency, is dynamic, portable, and carries no radiation risk. It should be the first choice and is typically sufficient for common pathologies such as appendicitis, intussusception, ovarian torsion, and hydronephrosis.
- Computed Tomography (CT): CT should be positioned as a "salvage tool" within the diagnostic pathway for pediatric acute abdomen, intervening only in cases where USG remains non-diagnostic, the clinical presentation is atypical, or there is a high suspicion of complications (e.g., abscess, necrosis, widespread mesenteric ischemia). CT's definitiveness is indispensable, particularly for the evaluation of bowel obstructions, retroperitoneal pathologies, and the grading of traumatic solid organ injuries.

The most significant limitation of CT is its use of ionizing radiation. Consequently, the necessity of every CT request must be rigorously questioned through strict collaboration between the radiologist and the clinician (2).

1.3. Radiation Risk and Dose Awareness (ALARA)

Children are inherently more susceptible than adults to the carcinogenic effects of radiation due to their rapidly dividing cell populations and longer life expectancy. The literature demonstrates that even at low-dose exposures (10–30mGy), a significant increase in long-term cancer risk may be observed (3).

With this high-risk awareness, radiologists must adopt the philosophy of "Best Image Quality at the Lowest Dose." This philosophy is embodied by the ALARA (As Low As Reasonably Achievable) principle, which forms the foundation of this chapter. The technical optimization strategies presented in the subsequent sections represent the practical application of this ethical responsibility. Avoiding unnecessary CT examinations and aggressively reducing the dose, even when the indication is clear, are core tenets of pediatric radiology.

2. PROTOCOL OPTIMIZATION and TECHNICAL IMPLEMENTATION

The use of Computed Tomography in pediatric acute abdomen patients necessitates the challenging balance of ensuring diagnostic adequacy against the long-term carcinogenic risk of ionizing radiation (the risk-benefit ratio). The key to achieving this balance lies in the meticulous application of advanced dose optimization techniques (4).

2.1. Fundamentals of Dose Optimization and ALARA Principle Application

Radiologists must adhere to the ALARA (As Low As Reasonably Achievable) principle as the guiding mandate for every pediatric CT examination. The practical implementation of this principle relies on a correct understanding of the dose metrics provided by the CT scanner:

- CTDIvol (Volumetric CT Dose Index): This metric represents the output of the radiation dose applied by the scanner for a specific protocol. It is the best reference parameter for protocol optimization.
- DLP (Dose-Length Product): DLP is the product of the CTDIvol value and the length of the scanned area. It shows the best correlation with the total radiation energy received by the patient and is used in the calculation of Effective Dose.

$$E\ (mSv) = DLP\ (mGy*cm) * k$$

Controlling the radiation dose always requires using protocols that are appropriate for the patient's age and Body Mass Index (BMI). Simply scaling down adult protocols generally leads to inadequate optimization.

2.2. Technical Parameter Settings and Low kVp Utilization

The conscious management of fundamental technical settings, which directly link image quality (noise, contrast) and dose, is

essential:

A. Low kVp Strategy

- **Rationale:** The most effective way to reduce the radiation dose (DLP) is by lowering the kVp value, as the dose is proportional to the square of the kVp.
- In pediatric patients, body diameters (especially in smaller children) and typically less fat tissue thickness are lower. This allows for the use of low voltage settings, such as 80-100 kVp.
- **Advantage:** Low kVp enhances contrast, particularly for iodine-based contrast agents, because the K-edge of iodine (33.2 keV) is closer to lower-energy photons. This allows for dose reduction while boosting diagnostic confidence in contrast- enhanced examinations.

B. Automatic Tube Current Modulation (ATCM)

- **Current (mA) Modulation:** ATCM systems (known by various trade names across different manufacturers) automatically adjust the tube current (mA) according to the patient's geometry (including angular, z-axis, and x/y-axis modulation).
  - By applying higher mA in thicker regions like the torso and lower mA in thinner anterior/posterior regions, ATCM maintains consistent image quality while preventing unnecessary radiation exposure.

2.3. Advanced Dose Reduction Techniques

A. Iterative Reconstruction (IR) Algorithms

Iterative Reconstruction (IR) has replaced the conventional Filtered Back Projection (FBP) method, effectively suppressing the noise that emerges in low-dose acquisitions, thereby enhancing image quality (5).

- **Working Principle:** IR operates by iteratively correcting the difference between the image estimate and the measured data. This method allows the required radiation dose to be reduced by 30% to 50% compared to FBP, while maintaining the same acceptable level of image quality.
- **Usage:** IR should be a cornerstone of pediatric protocols, ensuring that image noise is kept at acceptable levels during low-dose acquisitions.

B. Dual-Energy CT (DECT) and Monochromatic Imaging

DECT systems offer the ability to differentiate the attenuation properties of materials (iodine, calcium) by acquiring images at two different energy spectra (typically low and high kVp).

- **Monochromatic Imaging:** Virtual monochromatic images can be derived from DECT data. Specifically, low-energy monochromatic images in the 40–70 keV range significantly amplify iodine contrast and, consequently, lesion conspicuity, thereby enabling a

reduction in the IV contrast dose or a more aggressive reduction in the overall radiation dose.

2.4. Contrast Agent Use and Single-Phase Protocols

A. Intravenous (IV) Contrast Agent

- **Indications:** Trauma (solid organ laceration), suspicion of abscess/collection, vascular pathologies (volvulus, ischemia), neoplasm, or complicated infections (pyelonephritis).
- **Single-Phase Protocol:** CT for pediatric acute abdomen should generally be limited to a single-phase (contrast-enhanced venous phase) acquisition. Unnecessary non- contrast and arterial phases must be excluded from the protocol as they contribute to needless dose escalation.

B. Oral and Rectal Contrast Agents

- **General Consensus:** In current practice, routine use of oral or rectal contrast is not recommended for the diagnosis of appendicitis, due to the high spatial resolution offered by modern CT scanners and protocols (6).
- **Necessity of Use:** Contrast agents should be reserved for very specific circumstances, such as high suspicion of bowel obstruction (particularly when volumetric information is critical) or for localizing areas of fistula/perforation. Their use should be avoided whenever possible, as they lead to delays and impose an additional burden on the patient (7).

3. SYSTEMATIC APPROACH to DIFFERENTIAL DIAGNOSIS on CT

Pediatric acute abdomen poses a "pattern recognition" challenge for the radiologist. The high spatial resolution of CT allows for the systematic elimination of a wide range of differential diagnoses. The assessment should be grouped according to specific organ systems.

3.1. Inflammatory and Infectious Conditions

A. Acute Appendicitis (AA)

CT can offer superiority over USG in cases of complicated and atypical appendicitis. The radiological findings for AA diagnosis (the presence of a single finding alone may not be sufficient) are as follows (8):

- **Enlarged Appendix:** The external diameter of the appendix measures >6-7 mm (especially if the lumen does not contain contrast or fluid/air) (Figure 1).
- **Appendiceal Wall Thickening and Enhancement:** Increased wall thickness and enhancement due to hyperemia following IV contrast administration (Figure 1).
- **Periappendiceal Stranding (Fat Inflammation):** Increased density (stranding) in the periappendiceal fat tissue due to edema. This is one of the most specific findings.
- **Appendicolith:** High-density calcification (stone) within the lumen (Figure 2).
- **Complications:** If perforation is suspected, findings should include free air in the right lower quadrant, extraluminal appendicolith,

phlegmon, or an **abscess collection**. An abscess typically appears as a low-attenuation mass with peripheral contrast enhancement.

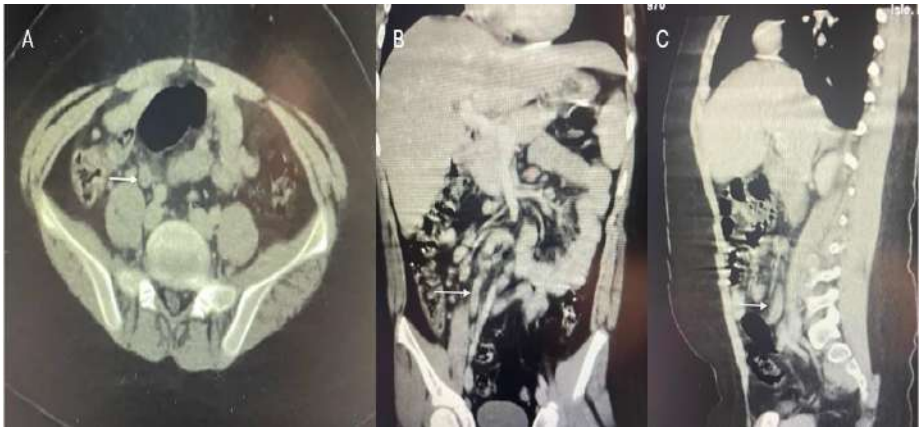

FIGURE 1: A 14-year-old male patient presented to the emergency department with right lower quadrant pain. An IV contrast-enhanced abdominal CT scan was performed. **A)** Axial image**s** demonstrate a dilated appendix with increased wall enhancement in the right lower quadrant of the abdomen. Increased density (stranding) in the periappendiceal fat tissue. **B)** Coronal images of the patient. **C)** Sagittal images of the patient.

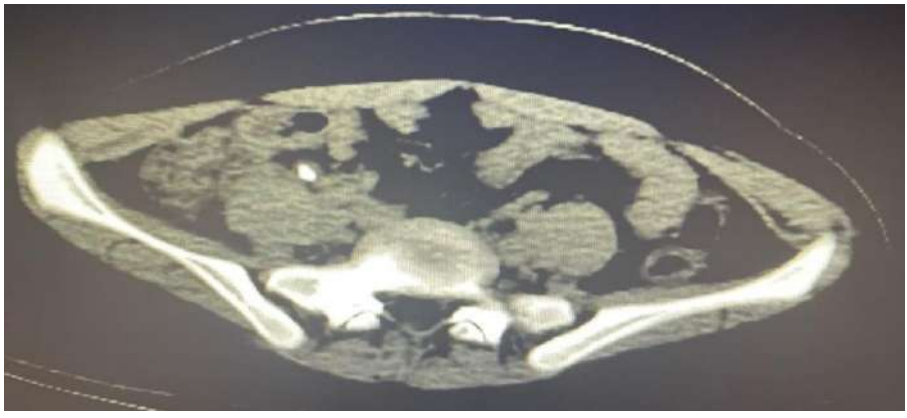

FIGURE 2: A 6-year-old female patient. Appendicolith: High-density calcification (stone) within the lumen in the right lower quadrant.

B. Mesenteric Lymphadenitis

This is a common, yet more benign, condition that mimics the clinical presentation of appendicitis (Figure 3).

- **Differentiating Criteria:** The presence of multiple lymph nodes measuring >5 mm in diameter in the right lower quadrant or ileocecal region, along with a normal-caliber appendix. Fat stranding may be less pronounced or entirely absent compared to appendicitis (9).

FIGURE 3: A 8-year-old female patient presented with right lower quadrant pain. A non-contrast abdominal CT scan was performed. The CT demonstrated several mesenteric lymph nodes in the right lower quadrant of the abdomen. The appendix appeared within normal limits.

C. Diverticulitis and Enterocolitis

- **Meckel Diverticulitis:** On CT, it may appear similar to appendicitis—a thickened, inflamed diverticulum in the right lower quadrant or distal ileum. Demonstrating a normal appendix is critical for differential diagnosis.
- **Inflammatory Bowel Disease (IBD) Flare-up: Crohn's Disease** typically demonstrates transmural wall thickening, mucosal hyperemia, and vascular engorgement known as the "Comb Sign."

3.2. Obstructive and Ischemic Pathologies

A. Intussusception

Intussusception is the most common cause of obstruction in children. Although USG is preferred, CT can aid in assessing the level of obstruction, its etiology (e.g., polyp, Meckel's diverticulum), and viability.

- **Findings:**

  - **Target Sign / Doughnut Sign:** A circular or target-like appearance seen on the transverse plane due to the telescoping bowel loops.
  - **Sausage Sign:** The appearance of an interdigitated mass seen on the longitudinal plane.
  - **Trapped Mesenteric Fat and Vessels:** Compressed and displaced mesenteric fat and vessels trapped within the intussusceptum.

B. Malrotation and Midgut Volvulus

This life-threatening condition involves the twisting of the small bowel around the **Superior Mesenteric Artery (SMA)** due to a short and abnormally positioned small bowel mesentery.

- **Critical Finding: Whirl Sign:** On CT, this appears as the **Superior Mesenteric Artery and Vein (SMV)** spiraling within the mesenteric fat. It is accompanied by the finding of the SMV positioned to the left of the SMA (normally it is to the right) and signs of obstruction (10).

3.3. Gynecological and Urinary Pathologies

A. Ovarian Torsion

Ovarian torsion is usually seen in adolescent girls. Due to diagnostic challenges, CT may sometimes be necessary.

- **Findings:** Significant enlargement (edema) of the torsed ovary, edema surrounding the fallopian tubes, and the **"Beak Sign"** resulting from the twisting of the vessels supplying the ovary. In cases of prolonged torsion, lack of contrast enhancement or heterogeneous enhancement (necrosis) may be observed in the ovary. Displacement of peripheral follicles is also a frequent finding (11).

B. Urolithiasis and Complicated Pyelonephritis

- **Urolithiasis:** Non-contrast CT is the gold standard for determining the location and density (Hounsfield Unit - HU) of stones. Low-dose protocols are sufficient for pediatric patients.

- **Pyelonephritis/Abscess:** In complicated urinary tract infections, CT is effective in demonstrating wedge-shaped or patchy enhancement defects in the renal parenchyma (Pyelonephritis) or fluid/necrotic collections (Abscess).

3.4. Trauma and Non-Traumatic Hemorrhage

CT is indispensable for the rapid and accurate grading of solid organ injuries in pediatric blunt abdominal trauma (12).

- **Findings:** Laceration (tear), subcapsular, or parenchymal hematomas in the liver, spleen, and kidney.
- **Active Hemorrhage (Spot Sign):** Extravasation of contrast material from an injured vessel into the peritoneal cavity during the venous phase. The presence of this finding is a critical prognostic factor in patients selected for Non-Operative Management.
- **Free Intraperitoneal Fluid (Blood):** Increased fluid attenuation (density) in the pelvis, hepatorenal (Morrison's pouch), and splenorenal spaces.

4. IMAGE QUALITY and REPORTING STANDARDS

Low-dose CT protocols implemented with radiation awareness inevitably introduce certain image quality limitations. The radiologist's duty is to manage these limitations without lowering the **diagnostic threshold**. Furthermore, clear and structured reporting is fundamental to improving the quality of communication with clinicians (13).

4.1. Low-Dose Limitations and Assessment Thresholds

The aggressive use of dose optimization techniques (especially very low kVp and mA values) leads to an unavoidable increase in noise and a relative reduction in image quality on CT scans. This situation can create difficulties in detecting small, low-contrast pathologies (14).

- **Artifacts and Noise Management:** While Iterative Reconstruction (IR) algorithms suppress noise, **subtle findings** like **minimal fat stranding** at tissue interfaces or thin fluid collections may be harder to visualize at very low dose levels compared to conventional Filtered Back Projection (FBP) images. The radiologist must employ windowing settings more carefully to detect these findings.
- **Diagnostic Threshold:** In low-dose CT, the threshold for specific findings, such as appendiceal wall thickening required to diagnose appendicitis, may not be as rigid as in high-dose protocols. For instance, the presence of periappendiceal stranding alone may be accepted as a sufficient finding for suspected appendicitis in a low-dose protocol, even when other findings (appendicolith or lumen diameter) are less conspicuous.

4.2. Structured Reporting

Rapid and clear communication is vital in emergency settings. Traditional free-text reporting methods carry the risk of omitting or misunderstanding clinically critical information. Therefore, Structured Reporting must be adopted for pediatric acute abdomen CT reports

(15).

- **Benefits:** Structured reporting enhances diagnostic certainty, ensures that critical findings (e.g., active hemorrhage, perforation, ovarian torsion) are mandatorily reported, and accelerates the surgical decision-making process.
- **Suggested Templates:** Reports should include major headings focused on the specific pathology:
  - **Imaging Technique:** Stating the dose parameters (CTDIvol, DLP) as evidence of radiation consciousness (e.g., "Low-dose pediatric protocol applied.").
  - **Critical Findings (Surgical Emergency):** Obstruction, active hemorrhage, organ rupture.
  - **Specific Assessment:**
    - **Appendicitis:** Appendiceal diameter, wall thickness, status of periappendiceal fat (stranding present/absent, severity).
    - **Obstruction:** Transition zone, level (small bowel/colon), cause (intussusception, volvulus).
    - **Ovaries:** Size, follicle location, enhancement status (suspicion of torsion).
  - **Differential Diagnosis:** Mesenteric lymphadenitis, IBD, urinary system pathologies.
  - **Impression:** A clear statement of the main diagnosis or the surgical emergency that has been excluded.

4.3. Significance of a Negative CT Scan (NPV)

A negative CT examination for acute abdomen provides significant reassurance to the clinician. CT is known to have a **high Negative Predictive Value (NPV)** for excluding major surgical causes of acute abdomen.

- **Clinical Application:** The reliable exclusion of surgical emergencies by CT allows the clinician to safely place the patient under observation or discharge them. The radiologist must clearly state this information in the report: *"No findings indicative of acute surgical abdomen were detected."* This provides the clinician with a scientific basis for avoiding unnecessary surgical intervention.

5. CONCLUSION and FUTURE PERSPECTIVES

5.1. Summary: Dose Awareness and Diagnostic Strategy

The management of pediatric acute abdomen remains a dynamic field for radiologists, requiring a constant balance between diagnostic certainty and ethical responsibility.

Computed tomography will continue to be an indispensable tool for cases where ultrasonography is inadequate or for complex pathologies. However, CT use must always be guided by an awareness of the radiation risks.

The central message of this chapter is the strict determination of the CT indication (using CT as a "salvage tool") and, in every examination:

- Utilization of precise low kVp settings and Automatic Tube Current Modulation,
- Adoption of Iterative Reconstruction (IR) algorithms as standard protocol,
- Implementation of single-phase contrast-enhanced acquisition strategies that eliminate unnecessary phases (e.g., non-contrast phase).

Radiologists must maintain a high Negative Predictive Value (NPV) for ruling out acute abdominal causes, even while applying the **ALARA** principle (13, 14).

5.2. Future Trends and Innovations

The field of pediatric imaging is undergoing continuous innovation aimed at further reducing the radiation dose and improving diagnostic reliability:

- **Algorithms Supported by Artificial Intelligence (AI) and Deep Learning:** AI has the potential to surpass current IR techniques by more effectively reducing noise or enhancing image quality in CT scans. Furthermore, automated diagnostic and measurement systems will help standardize diagnostic accuracy (16, 17).
- **Photon Counting Detectors (PCD) and Spectral CT:** Advanced detector technologies, such as PCD and Dual-Energy CT systems, promise better contrast and spatial resolution at lower radiation doses. These systems offer the potential to minimize contrast agent usage in the future.

- **The Increasing Role of MRI:** Due to its non-ionizing nature, Fast MRI protocols are increasingly accepted, especially for atypical cases of ovarian torsion and appendicitis, and may further narrow the indications for CT in the future (18).

The future of pediatric radiology will be shaped by our ability to utilize technology in a safer and smarter way.

6. REFERENCES

1. **Goske, M. J., et al.** (2012). The Image Gently campaign: working together to change practice. *American Journal of Roentgenology (AJR)*.
2. **Barth, R. A., s Otjen, J. P.** (2016). Imaging the Acute Abdomen in Children.
   Radiology Clinics of North America.
3. **Pearce, M. S., et al.** (2012). Radiation exposure from CT scans in childhood and subsequent risk of leukaemia and brain tumours: a retrospective cohort study. *The Lancet*.
4. **Strauss, K. J., s Goske, M. J.** (2011). Computed tomography and the appropriately lowered dose: a practical approach. *Pediatric Radiology*.
5. **Goksel, E. H., et al.** (2019). Technical aspects of pediatric CT: Dose optimization and iterative reconstruction. *European Journal of Radiology*.
6. **Patel, P. N., et al.** (2015). Utility of oral contrast in the evaluation of appendicitis in children with an optimized CT protocol. *Emergency Radiology*.
7. American College of Radiology (ACR) Appropriateness Criteria
8. **Hryhorczuk, A. L., et al.** (2019). Imaging of Acute Appendicitis in Children: An Update for the 21st Century. *Radiologic Clinics of North America*.
9. **Park, N. H., et al.** (2017). Differentiation of acute appendicitis from terminal ileitis using CT: focus on the periappendiceal fat. *European Radiology*.
10. **Epelman, M., et al.** (2015). The Pediatric Acute Abdomen: An Imaging Review.
    Radiographics.
11. **Servaes, S., et al.** (2017). Ovarian Torsion: Pearls and Pitfalls in Imaging

Diagnosis. *Pediatric Radiology*.

12. **Notrica, D. M., et al.** (2014). The American Association for the Surgery of Trauma (AAST) grading scale for pediatric splenic injury: a refinement. *Journal of Trauma and Acute Care Surgery*.
13. **Podgorsak, M. B., et al.** (2018). Practical applications of iterative reconstruction in pediatric CT. *Applied Clinical Informatics*.
14. **Brenner, D. J., et al.** (2013). Projected risks of cancer from exposure to medical radiation in US pediatric CT and fluoroscopy examinations. *AJR*.
15. ACR Structured Reporting Template for CT for Suspected Appendicitis in Children.
16. **Vining, D. J., s Leng, S.** (2018). Photon-counting CT: Technical principles and clinical applications. *Pediatric Radiology*.
17. **Brady, T. J., s Patz, S.** (2020). Artificial Intelligence and Deep Learning in Pediatric Imaging. *Pediatric Radiology*.
18. **Hernandez, A., s Lee, E. Y.** (2017). Fast MRI for Pediatric Acute Abdomen: Pearls and Pitfalls. *Radiographics*.

CHAPTER 4

IMAGE-GUIDED INTERVENTIONS IN PEDIATRIC RADIOLOGY

Specialist Dr. Ali CANTÜRK

1-INTRODUCTION

Interventional radiology (IR) has become an essential component of contemporary pediatric imaging and clinical care. As minimally invasive therapies continue to expand, pediatric IR now provides definitive or adjunctive treatment options for a broad spectrum of childhood diseases. Unlike adults, children have smaller anatomy, distinct physiology, limited physiological reserve, and significantly higher sensitivity to radiation. These differences require imaging protocols, procedural planning, and technical execution that are specifically adapted to the pediatric population (Chaudry vd., 2016).

General radiologists are frequently the first physicians to identify conditions that may benefit from an interventional approach.

Many pediatric IR referrals arise directly from ultrasound, CT, or MRI examinations interpreted in the radiology department. For this reason, general radiologists must understand which imaging findings indicate the need for IR referral, how to optimize imaging for pre-procedural planning, which modalities best characterize vascular or lymphatic anomalies, how to recognize complications after IR procedures, and how to effectively communicate with the interventional team.

Pediatric IR encompasses a wide range of procedures, including the management of vascular malformations, treatment of traumatic hemorrhage, image-guided gastrostomy and gastrojejunostomy placement, central venous access, lymphatic interventions, tumor ablation, and catheter-directed therapy for venous thrombosis. Although these procedures are performed by specialized pediatric interventional radiologists, the decision-making process begins with imaging, and general radiologists play a pivotal role in guiding evaluation.

2-Imaging Principles in Pediatric Interventional Radiology

Imaging forms the foundation of pediatric interventional radiology, and the decisions made by general radiologists directly influence procedural success, complication avoidance, and patient outcomes. Children present unique challenges stemming from their smaller anatomy, increased radiosensitivity, variable cooperation, and distinct disease patterns. Therefore, imaging approaches must be specifically adapted to pediatric physiology, emphasizing radiation reduction, high-resolution soft-tissue evaluation, and accurate characterization of vascular and lymphatic flow. The general radiologist's ability to recognize imaging patterns that necessitate interventional referral is essential, as most IR consultations originate from ultrasound, CT, or MRI examinations performed in the diagnostic department (Chaudry vd., 2016).

Ultrasound remains the first-line modality in pediatric IR because it provides real-time assessment without radiation exposure. It is

especially valuable in neonates and infants, where high-frequency transducers allow exquisite visualization of superficial structures and Doppler analysis reveals critical hemodynamic signatures. Low-flow lesions such as venous malformations demonstrate compressible, tubular or lacelike channels with slow or absent Doppler flow, while high-flow lesions such as arteriovenous malformations exhibit high-velocity arterial inflow and early venous filling. For lymphatic malformations, ultrasound allows differentiation between macrocystic lesions and microcystic lesions. These distinctions are fundamental to determining whether a child is likely to benefit from sclerotherapy, embolization, or another interventional approach (Paltiel vd., 2000).

Doppler interrogation plays a pivotal role in flow characterization, which is the single most important parameter guiding interventional decision-making. Identifying a high-flow shunt on Doppler fundamentally alters management, directing the radiologist toward angiographic evaluation and potential embolization rather than sclerotherapy.

Conversely, the absence of arterialized flow favors treatment with sclerosing agents. These determinations hinge on careful assessment of velocity patterns, resistance indices, and venous filling dynamics, all of which should be explicitly mentioned in the radiology report (Nosher vd., 2014).

Figure 1. Low-flow venous malformation: clinical, ultrasound, and CT correlation.

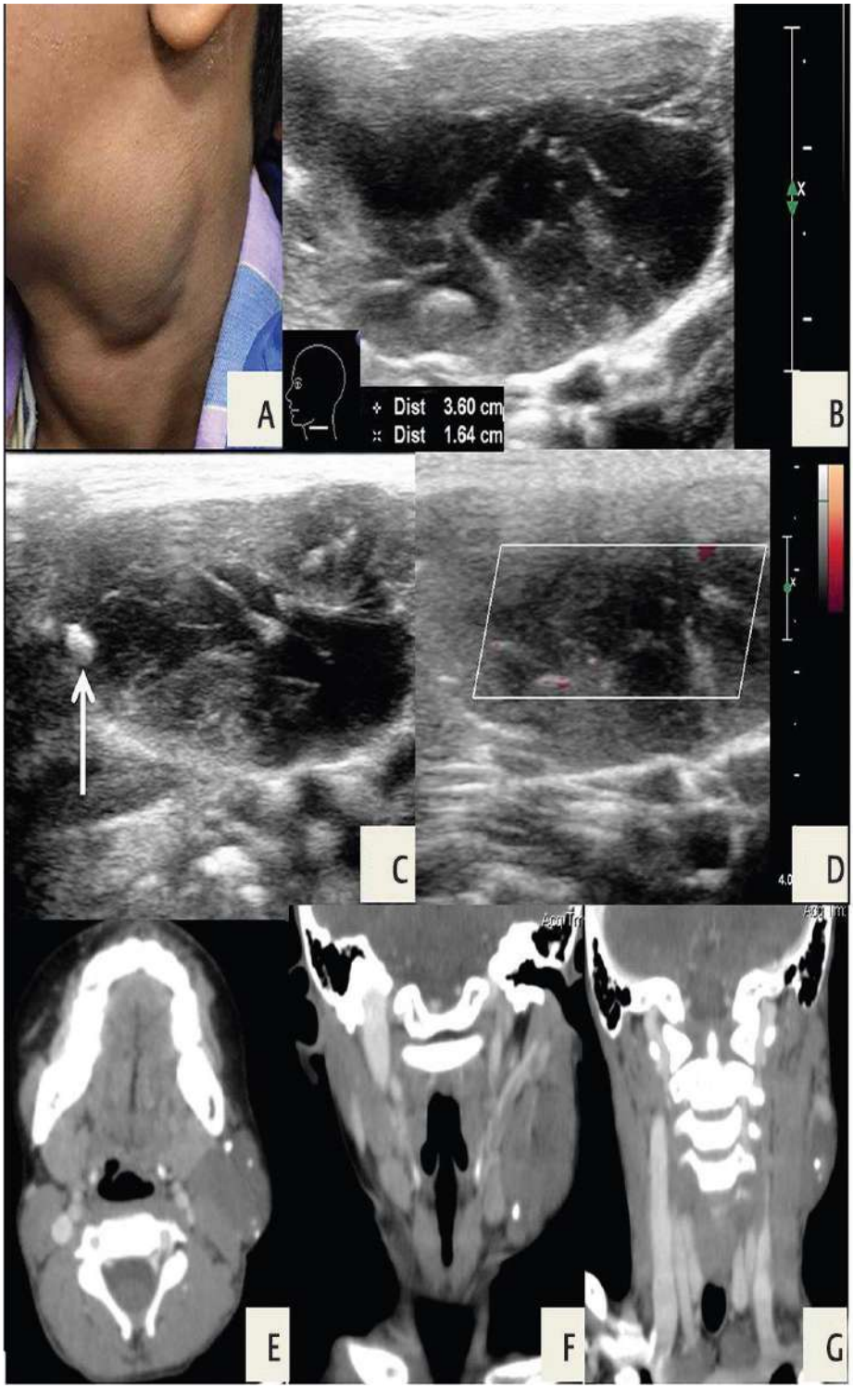
A
Dist 3.60 cm
Dist 1.64 cm
B
C
D
E
F
G

(A) Clinical photograph demonstrating a soft, compressible, non-pulsatile cervical swelling consistent with a low-flow vascular lesion.

(B) Gray-scale ultrasound showing a lobulated, heterogeneously echogenic lesion within the soft tissue of the neck.

(C) Longitudinal ultrasound image demonstrating multiple serpiginous channels with internal echogenic foci (arrow), compatible with phleboliths.

(D) Color Doppler ultrasound revealing minimal internal vascularity, a characteristic feature of low-flow venous malformations.

(E–G) Axial and coronal contrast-enhanced CT images showing a well-defined, hypodense soft-tissue mass with phleboliths and no evidence of arterial enhancement, supporting the diagnosis of a low-flow venous malformation.(Reproduced from *Mittal et al., Indian Journal of Radiology and Imaging*, 2021;31(4):1005–1023.)

Figure 2. High-flow arteriovenous malformation: clinical, ultrasound, Doppler, and CT correlation

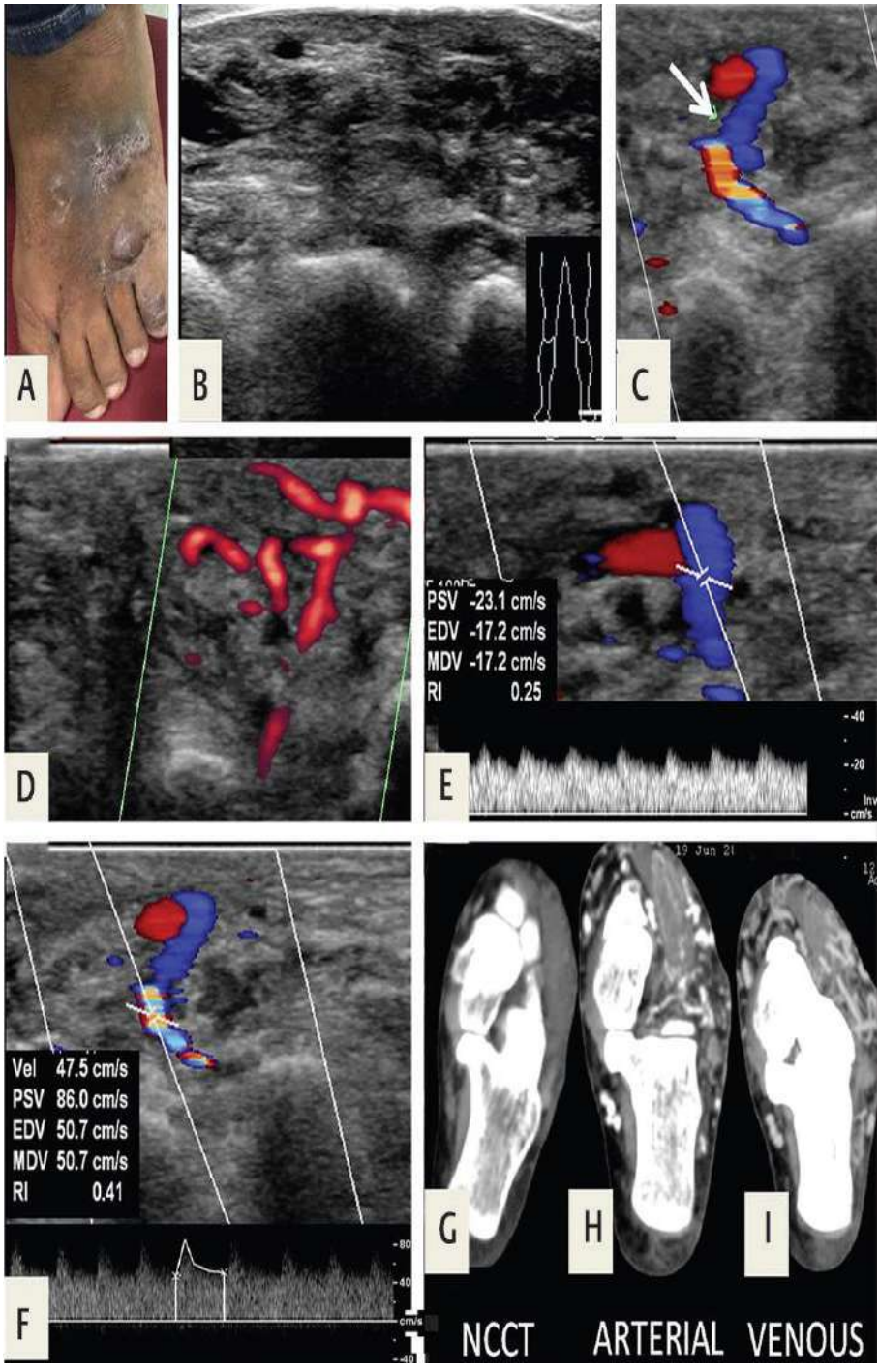
A
B
C
D
PSV -23.1 cm/s
EDV -17.2 cm/s
MDV -17.2 cm/s
RI 0.25
E
Vel 47.5 cm/s
PSV 86.0 cm/s
EDV 50.7 cm/s
MDV 50.7 cm/s
RI 0.41
F
G
H
I
NCCT
ARTERIAL
VENOUS

(A) Clinical photograph showing a soft-tissue swelling over the dorsal aspect of the foot with overlying skin discoloration, suggestive of an underlying vascular lesion.

(B) Gray-scale ultrasound image depicting a heterogeneous soft-tissue abnormality without a discrete mass, raising suspicion for a vascular etiology.

(C) Color Doppler ultrasound demonstrating a large, tortuous vascular channel with aliasing (arrow), consistent with high-velocity arterialized flow.

(D) Additional Doppler imaging showing multiple serpiginous, dilated vascular channels typical of arteriovenous shunting.

(E) Spectral Doppler waveform obtained from a draining vein illustrating arterialized venous flow with low resistance (RI = 0.25) and high diastolic velocities—hallmark features of a high-flow AVM.

(F) Spectral Doppler waveform from the feeding artery revealing increased peak systolic velocity (PSV = 86 cm/s) and marked diastolic flow (low RI = 0.41), confirming a high-flow vascular malformation.

(G–I) Axial CT images (non-contrast, arterial phase, venous phase) demonstrating a hypervascular soft-tissue lesion with early arterial enhancement and persistent venous opacification, characteristic of

high-flow arteriovenous malformations. (Reproduced from *Mittal et al., Indian Journal of Radiology and Imaging*, 2021;31(4):1005–1023.)

Imaging Principles in Pediatric Interventional Radiology

Fluoroscopy remains central to many pediatric interventional radiology (IR) procedures, including gastrointestinal access, sclerotherapy, embolization, and lymphangiography. Because children are disproportionately sensitive to ionizing radiation, all procedures must strictly adhere to pediatric radiation protection principles. Dose reduction strategies include the use of pulsed fluoroscopy at the lowest feasible frame rates, tight collimation, minimization of magnification, pediatric-specific fluoroscopy presets, last image hold, and removal of anti-scatter grids in small children. These measures are essential for both intraprocedural guidance and preparatory steps such as contrast opacification of venous or lymphatic malformations **(ICRP, 2013)**.

MRI provides superior soft-tissue contrast and is the imaging modality of choice for comprehensive evaluation of vascular and lymphatic anomalies. T2-weighted imaging delineates fluid-rich components of lymphatic malformations, while T1-weighted and post-contrast fat-suppressed sequences characterize hemorrhage, proteinaceous content, and enhancement patterns. Venous malformations typically appear as lobulated lesions with internal septations, delayed progressive enhancement, and signal voids corresponding to phleboliths. Arteriovenous malformations demonstrate serpiginous flow voids and early arterial enhancement on dynamic MR angiography, allowing precise identification of the nidus and shunting physiology. MR-based

lymphatic imaging techniques have further expanded noninvasive evaluation of central lymphatic anatomy and leakage patterns, supporting targeted interventional planning **(Itkin ve Nadolski, 2018)**.

Although CT is used sparingly in pediatric populations because of ionizing radiation exposure, it plays a critical role in selected clinical scenarios. In trauma, CT is the most accurate modality for detecting solid-organ injury, retroperitoneal hematomas, and active arterial extravasation, findings that may necessitate urgent embolization. CT angiography is also valuable for evaluating suspected vascular injury, arterial dissection, or complex high-flow lesions when ultrasound or MRI are inconclusive. Additionally, CT provides superior assessment of osseous involvement and calcified components in venous malformations **(Flors vd., 2011)**.

Appropriate imaging selection requires a systematic, child-centered approach. Ultrasound generally serves as the initial modality, MRI provides definitive lesion characterization, fluoroscopy enables image-guided intervention with careful dose management, and CT is reserved for urgent or anatomically complex situations.

The radiologist's role is to integrate clinical presentation with imaging findings to identify conditions that warrant interventional referral, such as imaging evidence of active hemorrhage, high-flow shunting, or lymphatic leakage.

3-Pediatric Vascular Anomalies

Vascular anomalies represent one of the most complex diagnostic categories in pediatric radiology and remain a major source of referral

to interventional radiology. Clinical presentations range from asymptomatic, compressible venous malformations to aggressive, high-flow arteriovenous malformations with destructive potential. Accurate classification is essential for determining prognosis and appropriate management. The contemporary framework for vascular anomalies is based on the biologic distinction between vascular tumors and vascular malformations, as formalized by the International Society for the Study of Vascular Anomalies (ISSVA). This classification differentiates lesions with endothelial proliferation from structural vascular anomalies lacking proliferative capacity **(Merrow vd., 2016)**.

3.1 ISSVA Classification and Clinical Relevance

The ISSVA classification separates vascular anomalies into vascular tumors and vascular malformations. Vascular tumors, such as infantile hemangiomas, exhibit characteristic phases of proliferation and involution and often respond to medical therapy. In contrast, vascular malformations are present at birth, grow proportionally with the child, and persist throughout life unless treated. Their clinical behavior is determined by the involved vessel type and, critically, by flow dynamics. Differentiation between low-flow malformations (venous and lymphatic) and high-flow malformations (arteriovenous) is fundamental, as flow characteristics directly guide interventional strategy, including sclerotherapy versus embolization **(Nosher vd., 2014)**.

3.2 Embryology and Pathophysiologic Basis

Vascular malformations arise from disruptions during vasculogenesis, angiogenesis, or vascular remodeling. Errors in these tightly regulated

developmental processes result in abnormal vessel differentiation and persistence. Advances in molecular genetics have identified recurrent somatic mutations in pathways such as PIK3CA, TEK/TIE2, and RASA1, explaining the progressive nature of many vascular malformations and supporting a shift toward biologically informed therapeutic approaches **(Ghosh vd., 2020)**.

3.3 Clinical Presentation and Disease Behavior

Clinical manifestations depend on vessel type, anatomic distribution, and flow pattern. Venous malformations typically present as soft, compressible, bluish lesions that enlarge with dependency or physical activity and may contain phleboliths. Intramuscular venous malformations can cause disproportionate pain and functional impairment. Lymphatic malformations present as macrocystic lesions with large septated fluid collections or as microcystic disease infiltrating the skin and subcutaneous tissues, often complicated by infection, leakage, or hemorrhage. High-flow arteriovenous malformations follow a distinct clinical course, often demonstrating warmth, pulsatility, bruit, and progressive tissue destruction, with advanced stages associated with high-output cardiac failure.

3.4 Imaging Evaluation

Imaging evaluation is central to diagnosis and management. Ultrasound is typically the first-line modality, with Doppler interrogation essential for flow assessment. Low-flow malformations demonstrate compressible hypoechoic channels with slow or absent Doppler signal, while high-flow lesions show arterialized waveforms and early venous filling. MRI provides comprehensive assessment of lesion extent,

compartmentalization, and flow characteristics. Catheter angiography remains the gold standard for high-flow malformations and serves as both a diagnostic and therapeutic tool **(Paltiel vd., 2000)**.

Figure 3. Fluoroscopic appearance of contrast-enhanced sclerosant injection in a slow-flow vascular malformation

Fluoroscopic image obtained during percutaneous sclerotherapy of a slow-flow vascular malformation located in the subcutaneous tissues of the forearm. Under ultrasound guidance, a needle was advanced into the lesion and contrast-mixed lauromacrogol 400 was gently injected, outlining the multilobulated venous channels without evidence of early venous drainage. This opacification pattern confirms the low-flow hemodynamic behavior and allows delineation of treatment compartments prior to sclerosant deposition.

3.5. Interventional Management of High-Flow Malformations

High-flow malformations require a fundamentally different therapeutic approach. Embolization must be directed toward the nidus rather than the feeding arteries alone; otherwise, the lesion will recur through collateral recruitment. Liquid embolic agents such as n-butyl cyanoacrylate (n-BCA) and ethylene-vinyl alcohol copolymer (Onyx) are central in contemporary practice. n-BCA polymerizes rapidly upon contact with blood, allowing deep nidus penetration when appropriately diluted with lipiodol. Onyx provides controlled, gradual penetration due to its non-adhesive properties, making it particularly useful for complex or compartmentalized AVMs **(Yakes vd., 1996)**. In many cases, treatment is staged, with sequential embolizations to protect surrounding tissue and reduce hemodynamic load. Surgical resection may be considered after adequate devascularization.

Figure 4. Follow-up T2-weighted MRI and X-ray correlation after Onyx embolization.

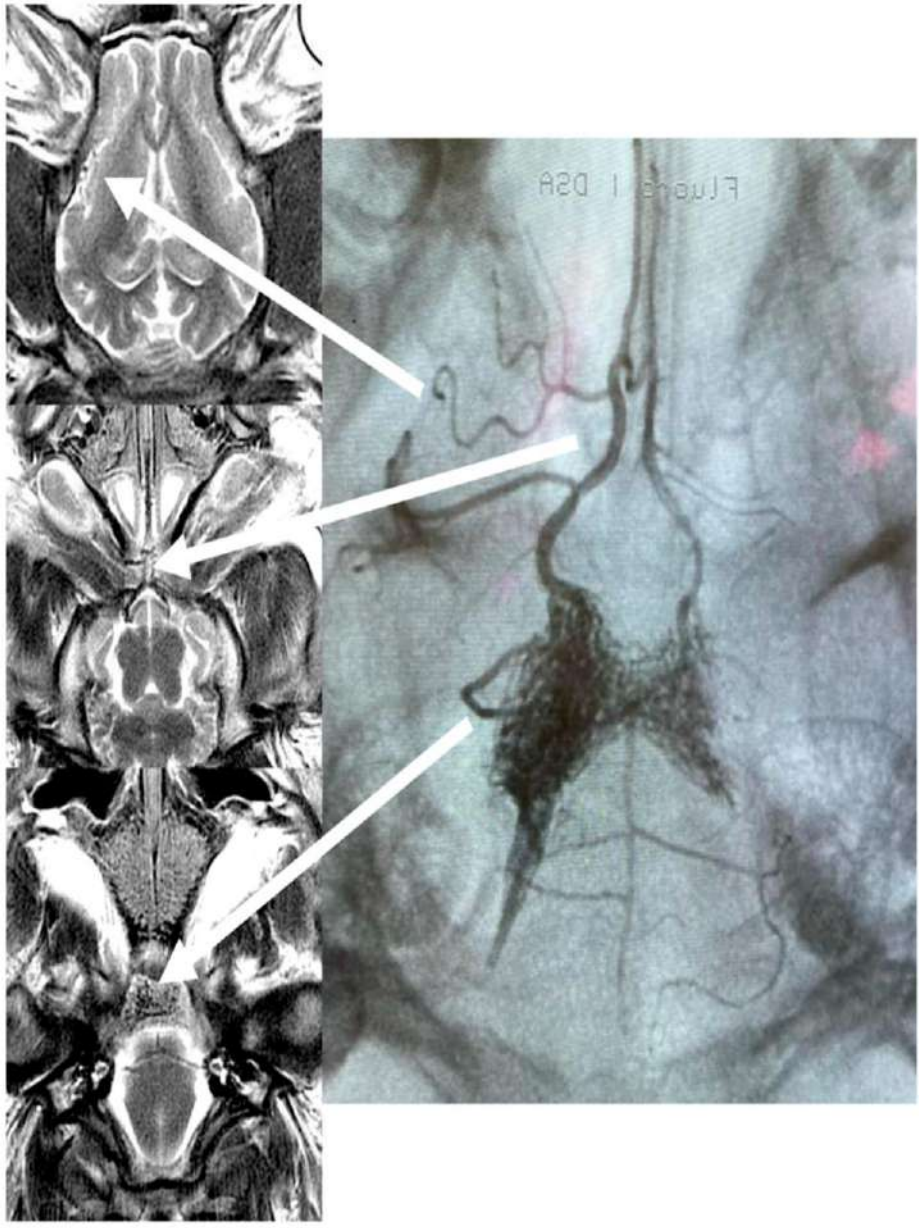

Follow-up T2-weighted MRI scans obtained 20 minutes after Onyx embolization demonstrate signal changes corresponding to the embolized arteriovenous malformation, with the absence of residual flow-related signal voids. The adjacent X-ray image depicts the radiopaque Onyx cast, outlining the treated nidus and confirming adequate filling of the malformation. Together, these modalities provide both anatomical and procedural confirmation of successful embolization (Zawadzki M, et al., Brain Sciences, 2023;13:915).

3.6 Syndromic Associations

Many vascular malformations occur in the context of syndromes, and radiologists should recognize the imaging patterns that prompt further evaluation. Klippel–Trenaunay syndrome combines capillary, lymphatic and venous malformations with limb overgrowth, while CLOVES syndrome demonstrates complex lymphatic and venous anomalies associated with truncal fatty overgrowth and somatic PIK3CA mutations. Parkes Weber syndrome features diffuse high-flow arteriovenous shunting and must be distinguished from other limb-overgrowth disorders. PTEN-related hamartoma syndromes and Sturge–Weber syndrome also include characteristic vascular involvement. Recognition of syndromic patterns is important because management requires coordinated multidisciplinary care, and interventional procedures may address only part of the disease spectrum (Bertino vd., 2019; Martínez-Lopez vd., 2017; Sánchez-Espino vd., 2023)**.**

3.7 Complications and Follow-Up

Complications vary with lesion type and treatment modality. Pain, swelling and temporary neuropathy are common after sclerotherapy. Ethanol poses risks of skin necrosis, nerve injury and cardiopulmonary collapse. Bleomycin carries a rare but important risk of pulmonary toxicity, although doses used in interventional radiology are typically far below thresholds associated with lung injury. Following embolization of high-flow lesions, radiologists should evaluate for non-target embolization, persistent nidus flow or tissue ischemia. Follow-up MRI at three to six months is recommended to assess treatment response and identify residual or recurrent disease. Long-term surveillance is essential, as many malformations progress during growth or hormonal transitions (Alomari, 2010;Nosher vd., 2014).

4. THE ROLE OF INTERVENTIONAL RADIOLOGY IN PEDIATRIC TRAUMA

Trauma represents one of the most time-critical areas in which interventional radiology (IR) significantly impacts pediatric outcomes. Although children demonstrate greater physiologic resilience and enhanced vasoconstrictive capacity compared with adults, rapid clinical deterioration may occur once compensatory mechanisms fail. For general radiologists, early recognition of imaging findings that warrant IR consultation is therefore fundamental to effective trauma management. Contrast-enhanced computed tomography (CT) plays a central diagnostic role in the evaluation of abdominal and pelvic trauma, offering high sensitivity for detecting solid-organ injuries,

retroperitoneal hematomas, vascular disruption, and active arterial contrast extravasation—findings that guide decisions regarding selective arterial embolization (Gaines, 2009).

Children most commonly sustain injuries to the spleen, liver, and kidneys following blunt abdominal trauma. While the majority of these injuries are managed non-operatively, the presence of active contrast extravasation—commonly termed an "arterial blush"—strongly correlates with ongoing hemorrhage and represents one of the most reliable imaging indicators for urgent IR involvement. Additional vascular findings such as pseudoaneurysm formation or arteriovenous fistulas further strengthen the indication for endovascular intervention. Selective embolization has demonstrated high technical success rates in pediatric patients, effectively controlling hemorrhage while preserving organ function and avoiding the morbidity associated with open surgery (Soto ve Anderson, 2012).

The spleen is the most frequently injured intra-abdominal organ in children, and splenic artery embolization has become an integral component of contemporary non-operative management algorithms. Proximal splenic artery embolization reduces intrasplenic perfusion pressure while maintaining immunologic function, making it particularly advantageous in pediatric patients. Distal embolization may be indicated when focal pseudoaneurysms or sites of active bleeding are identified. Accordingly, radiology reports should describe not only the injury grade but also the presence or absence of active extravasation, vascular irregularity, or pseudoaneurysm formation, as these findings directly influence IR strategy.

Liver trauma similarly benefits from an IR-centered approach. Hepatic arterial embolization is indicated when CT demonstrates active extravasation, pseudoaneurysm formation, or expanding hematoma despite relative hemodynamic stability. Renal injuries are most often treated conservatively; however, large perirenal hematomas, segmental devascularization, or vascular injuries may necessitate selective embolization. Recognition of arterial dissection or segmental arterial occlusion is particularly important, as these findings may require targeted endovascular therapy (Gaines, 2009).

Pelvic trauma is less common in children than in adults but carries a high risk of life-threatening hemorrhage when present, typically reflecting high-energy mechanisms. Active arterial bleeding from branches of the internal iliac system identified on CT should prompt immediate IR consultation.

Endovascular embolization allows rapid hemorrhage control with substantially lower morbidity compared with open pelvic packing. Importantly, general radiologists must differentiate true arterial extravasation from venous oozing, which often appears as delayed, lower-attenuation contrast pooling and generally does not require urgent intervention.

Thoracic trauma may also necessitate IR involvement in selected cases. While traumatic hemothorax is usually managed with tube thoracostomy, persistent bleeding may indicate injury to intercostal or internal mammary arteries, particularly in association with posterior rib fractures.

In such scenarios, contrast-enhanced CT followed by targeted arterial embolization can effectively control hemorrhage and obviate the need for thoracotomy (Matsen vd., 2013).

Across all trauma scenarios, the role of the general radiologist extends beyond injury detection alone. Radiology reports should clearly document the presence or absence of arterial contrast extravasation, pseudoaneurysm formation, arteriovenous fistulas, segmental devascularization, expanding hematomas, and associated fractures. These findings enable trauma surgeons and interventional radiologists to rapidly establish a coordinated management plan.

Follow-up imaging after embolization is typically performed using ultrasound or CT, depending on the injured organ and clinical stability, with emphasis on identifying expected post-embolization changes and excluding new vascular complications.

Long-term outcomes are generally excellent, with high rates of organ preservation when pediatric trauma is managed using selective embolization.

Figure 5. Spleen laceration (grade 4- AAST clasification)

A grade 4 splenic laceration, with several parenchymal fracture lines, is present and there is evidence of active arterial extravasation from the anterior aspect of laceration. A moderately large amount of free intra-abdominal fluid is present.

Figure 6. Coil embolisation of splenic artery pseudoaneurysm

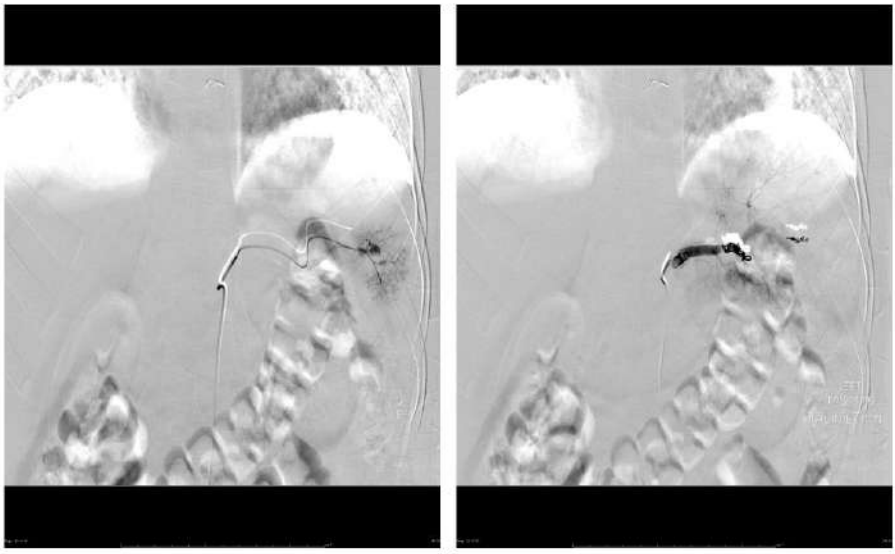

Mid pole splenic artery pseudoaneurysm. No active bleeding at the time of angio.

Progreat microcatheter used. Pseudoaneurysm excluded with 5 of 2 x 5mm Figure-8-Pushable-0.14 coils. Main Splenic artery embolized at the hilum, using 5 of 5 x 40mm Helical-35- Pushable coils.

(Case courtesy of RMH Core Conditions, Radiopaedia.org, rID: 28448)

Gastrointestinal System Interventions in Pediatric Patients

Gastrointestinal access procedures constitute one of the most frequently performed nonvascular interventions in pediatric interventional radiology. Their clinical relevance stems from the large population of children requiring long-term enteral nutrition because of neurologic impairment, congenital anomalies, metabolic disorders, or chronic

gastrointestinal dysfunction. Although percutaneous gastrostomy and gastrojejunostomy (GJ) are well-established techniques across all age groups, their application in children requires careful consideration of anatomy, sedation requirements, and procedure-specific complications. Because general radiologists frequently perform the initial abdominal imaging and identify anatomic constraints, familiarity with the indications, imaging principles, and potential pitfalls of these procedures is essential.

The foundation of radiologically guided gastrostomy is the creation of a safe percutaneous tract into the stomach under imaging guidance. Fluoroscopy has traditionally served as the primary modality, while ultrasound plays an important adjunctive role in confirming gastric apposition and identifying a safe access window between the abdominal wall and adjacent bowel loops. Children with neurologic impairment frequently exhibit gastroparesis, gastroesophageal reflux, scoliosis, or altered abdominal anatomy, all of which may increase procedural complexity. Pre-procedural ultrasound can identify interposed colon or small bowel and help determine whether gastric insufflation will provide adequate anterior wall apposition (Sidhu vd., 2010).

Radiologic gastrostomy typically begins with gastric insufflation via a nasogastric tube, which displaces adjacent organs and brings the stomach into contact with the anterior abdominal wall. After confirmation of a safe access window, gastropexy anchors are deployed to secure the stomach and reduce the risk of leakage or peritonitis. Under fluoroscopic guidance, a needle is advanced into the stomach, followed by guidewire placement, tract dilation, and insertion of the

gastrostomy tube. Final tube position is confirmed by contrast injection, demonstrating intragastric opacification without extraluminal leakage. Recognition of appropriate fluoroscopic positioning is critical to minimizing complications.

Gastrojejunostomy placement is indicated in children who cannot tolerate gastric feeding because of severe reflux, recurrent aspiration, or gastroparesis. The procedure involves advancing a catheter or tube through the pylorus into the proximal jejunum under fluoroscopic guidance. In children, the duodenal sweep is often mobile and acutely angled, necessitating gentle manipulation and use of small-caliber catheters to avoid mucosal injury. Radiologists must recognize the expected fluoroscopic position of the jejunal limb and identify malposition, such as retrograde looping into the stomach or failure to traverse the pylorus **(**Funaki vd., 1997**).**

Complications of gastrostomy and GJ placement range from minor to life-threatening, and imaging plays a central role in early detection. Minor complications include peristomal cellulitis, hypergranulation tissue, and tube dislodgement. Major complications include peritonitis due to intraperitoneal leakage, gastric outlet obstruction from overinflated balloons, and buried bumper syndrome. Children with severe malnutrition or inadequate gastric distention are at increased risk of intraperitoneal tube placement. When malposition is suspected, fluoroscopic contrast studies or radiographs are essential for identifying extraluminal contrast, peri-tubal collections, or failure of contrast to enter the stomach.

Long-term maintenance and follow-up imaging are equally important. As children grow, gastrostomy tubes often require upsizing or exchange. Radiologists may be asked to assess tube patency, balloon integrity, or tract maturation prior to replacement. In children with GJ tubes, retrograde migration of the jejunal limb into the stomach is common and may result in feeding intolerance or aspiration. Contrast studies remain the most reliable method for evaluating tube configuration, while ultrasound or CT may be required in cases of suspected abscess, buried bumper syndrome, or high-grade obstruction (Lorenz, 2011).

Non-fluoroscopic imaging modalities increasingly support procedural planning and complication assessment. Ultrasound is particularly useful in children with prior abdominal surgery or complex anatomy, while cross-sectional imaging may reveal gastric volvulus, malrotation, or congenital anomalies that necessitate modification of technique or preclude percutaneous access altogether.

Ultimately, gastrostomy and gastrojejunostomy procedures exemplify the multidisciplinary nature of pediatric interventional care. Radiologists contribute not only through technical execution but also through pre-procedural anatomic assessment, identification of risk factors, device selection, and post-procedural surveillance. This role is especially critical in children with complex medical conditions who depend on durable gastrointestinal access for growth and development

Figure 7.

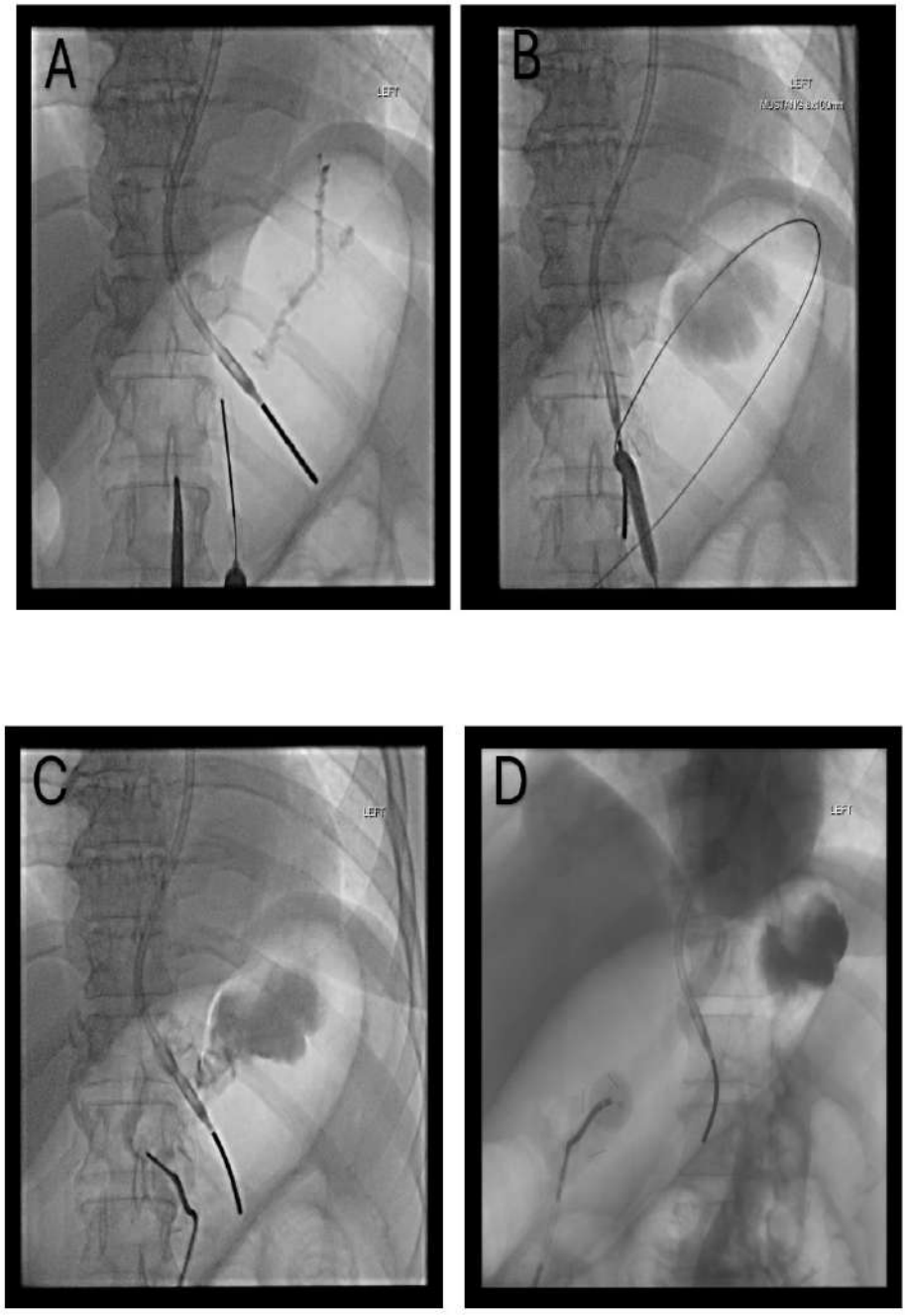

(A): Gastric insufflation through the nasogastric tube demonstrates adequate distension, allowing safe selection of an access window.
(B): Balloon dilation of the percutaneous tract is performed over the guidewire under fluoroscopic guidance to create a stable channel for gastrostomy placement.
(C): Contrast injection through the newly inserted gastrostomy tube confirms intragastric positioning and excludes extraluminal leak.
(D): Final fluoroscopic image demonstrates the gastrostomy tube in satisfactory position, with appropriate balloon inflation securing the device within the stomach.
(Case courtesy of Craig Hacking, Radiopaedia.org, rID: 188234)

CONCLUSION

Pediatric interventional radiology has evolved into a vital extension of both diagnostic imaging and therapeutic care, offering minimally invasive solutions for a spectrum of vascular, hepatobiliary, lymphatic, genitourinary, oncologic and traumatic conditions in children. Its growth reflects advances in imaging technology, device miniaturization and procedure specific expertise tailored to pediatric anatomy and physiology. Throughout this chapter, emphasis has been placed on equipping general radiologists with a foundational interventional perspective recognizing disease patterns, identifying imaging findings that require intervention, and understanding the principles underlying major IR procedures.

The partnership between diagnostic and interventional radiology is especially important in children, whose long-term outcomes depend on accurate imaging, minimally invasive treatment and careful follow-up. From vascular malformations to biliary strictures, from tumor biopsy to nephrostomy access, each interventional pathway begins with imaging interpretation. Radiologists therefore play a central role not only in diagnosis but also in directing patients toward the most effective and often least invasive therapy.

As pediatric IR continues to expand, general radiologists who understand these principles will be better equipped to participate in multidisciplinary decision-making, guide appropriate referral and improve patient outcomes. This integration of diagnostic and interventional expertise represents the future of pediatric radiological care and underscores the importance of continued collaboration, education and innovation within the field.

REFERENCES

Chaudry G. Paediatric interventional radiology. South African Journal of Radiology. 2016;20(1):a940. doi:10.4102/sajr.v20i1.940.

Paltiel HJ, Burrows PE, Kozakewich HPW, Mulliken JB. Soft-tissue vascular anomalies: utility of ultrasound for diagnosis. *Radiology.* 2000;214(3):747–754. doi:10.1148/radiology.214.3.r00mr21747.

Nosher JL, Murillo PG, Liszewski M, Gendel V, Gribbin C. Vascular anomalies: a pictorial review of nomenclature, diagnosis, and treatment. *World Journal of Radiology.* 2014;6(9):677–692. doi:10.4329/wjr.v6.i9.677.

ICRP. Radiological protection in paediatric diagnostic and interventional radiology. *ICRP Publication 121*. Ann ICRP. 2013;42(2):1–63.

Itkin M, Nadolski GJ. Modern techniques of lymphatic imaging and interventions. *J Vasc Interv Radiol.* 2018;29(4):506–517.

Flors L, Leiva-Salinas C, Maged IM, et al. MR imaging of soft-tissue vascular malformations: diagnosis, classification, and therapy follow-up. *Radiographics.* 2011;31(5):1321–1340.

Merrow AC, Gupta A, Patel MN, Adams DM. 2014 revised classification of vascular lesions from the International Society for the Study of Vascular Anomalies. *Radiographics.* 2016;36(5):1494–1516.

Nosher JL, Murillo PG, Liszewski M, Gendel V, Gribbin C. Vascular anomalies: a pictorial review of nomenclature, diagnosis and treatment. *World J Radiol.* 2014;6(9):677–692.

Ghosh P, et al. Vascular anomalies. *Nat Rev Dis Primers.* 2020;6:65.

Paltiel HJ, Burrows PE, Kozakewich HPW, Mulliken JB. Soft-tissue vascular anomalies: utility of ultrasound for diagnosis. *Radiology.* 2000;214(3):747–754.

Yakes WF, Rossi P, Odink H. *How I do it: arteriovenous malformation management.* J Vasc Interv Radiol. 1996;7(6):805–817.

Bertino F, Braithwaite KA, Hawkins CM, Gill AE, Briones MA, Swerdlin R, et al. Congenital limb overgrowth syndromes associated with vascular anomalies. *Radiographics.* 2019;39(2):491-515. doi:10.1148/rg.2019180136. P

Martínez-Lopez A, Blasco-Morente G, Pérez-Lopez I, Herrera-Garcia JD, Luque-Valenzuela M, Sánchez-Cano D, et al. CLOVES syndrome: review of a PIK3CA-related overgrowth spectrum (PROS). *Clin Genet.* 2017;91(1):14-21. doi:10.1111/cge.12832.

Sánchez-Espino LF, Ivars M, Antoñanzas J, Baselga E. Sturge-Weber syndrome: a review of the pathophysiology, genetics, clinical features and current management approaches. *Ther Adv Chronic Dis.* 2023;16:63-81. doi:10.2147/TACG.S363685.

Alomari AI. Percutaneous sclerotherapy for vascular malformations. *Semin Intervent Radiol.* 2010;27(3):276–285.

Nosher JL, Murillo PG, Liszewski M, Gendel V, Gribbin C. Vascular anomalies: a pictorial review of nomenclature, diagnosis and treatment. *World J Radiol.* 2014;6(9):677–692.

Gaines BA. *Selective nonoperative management of blunt splenic injury in children.* Pediatr Radiol. 2009;39(10):1034–1039.

Soto JA, Anderson SW. *Multidetector CT of blunt abdominal trauma.* Radiology. 2012;265(3):678–693.

Matsen SL, et al. *Intercostal artery embolization for traumatic hemothorax in children.* J Pediatr Surg. 2013;48(8):1733–1738.

Sidhu MK, Coley BD, Anton CG, et al. Image-guided percutaneous gastrostomy in children: role of ultrasound. *Pediatr Radiol.* 2010;40:1439–1446. doi:10.1007/s00247-009-1468-3.

Funaki B, Zaleski GX, Leef JA, et al. Percutaneous gastrojejunostomy tube placement: techniques and results. *Radiology.* 1997;205(3):673–679.

Lorenz JM. Percutaneous gastrostomy and gastrojejunostomy in children. *Semin Intervent Radiol.* 2011;28(3):273–284

PEDIATRIC ABDOMINOPELVIC CYSTIC MASSES: IMAGING FINDINGS AND TREATMENT APPROACHES

Dr. Büşra Şeker

INTRODUCTION

Congenital or acquired cystic abdominal masses are common in the pediatric population. These lesions usually present with similar clinical symptoms such as abdominal distention, bowel obstruction, palpable mass, swelling, and etc.. Both clinical findings and imaging modalities can significantly help to determine the diagnosis, further characterization, management, and presurgical planning. Here we describe the characteristic imaging findings of various pediatric abdominal cystic masses arising from the liver, biliary tract, pancreas, spleen, kidney, bowel, mesentery, pelvic cavity, and miscellaneous tissues.

1. HEPATOPANCREATICOBILIARY SYSTEM

1.1. Hepatic Mesenchymal Hamartoma (HMH)

HMH is a benign hamartomatous developmental malformation in the liver with unknown etiology. HMH typically occurs in children and neonates, with most cases present within the first two years of life (80%) and there is male predominance (2:1). Pathologically, it is characterized by a combination of epithelial structures in myxoid of fibrous stroma with fluid accumulation mean of lymphangiomatous channels. HMH forms are multilocular cystic, cystic with a solid component, or less commonly predominantly solid. Patients present

with an enlarging abdominal mass without tenderness, free fluid, jaundice, and congestive heart failure due to vena cava inferior compression. 80% arise in the right lobe of the liver and 20% are pedunculated. On ultrasound (US), usually well-defined complex cystic mass containing both varying size cystic and solid components are shown. This tumor is avascular centrally and frequently contains septations. Solid components are hyperechoic compared with liver parenchyma. On computed tomography (CT), findings depend on the amount of stromal tissue which show contrast enhancement while the cystic component does not. Displacement of intrahepatic vascularite may be seen because of HMH, which is an important finding for differential diagnosis. On magnetic resonance imaging (MRI), lesions can be seen hyperintense on T2 weighted (T2W), while T1 weighted (T1W) signal can be hypointense or hyperintense due to the amount of water or protein contents. On treatment, provided to the literature, HMH shows spontaneous regression with medical therapy but surgical resection is usually preferred, especially in larger lesions due to increased risk of malignancy and mass effect such as vena cava inferior obstruction, heart failure, and etc..

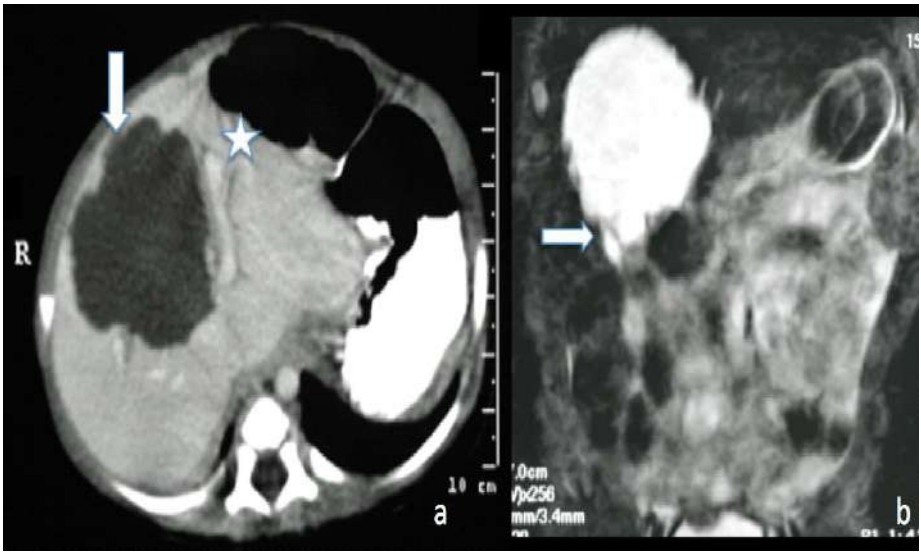

Figure 1: Hepatic Mesenchymal Hamartoma. A cystic lesion with septa (figure b) that creates a protrusion in the vascular structure (figure a, star) is seen in the right lobe of the liver.

1.2. Hepatic Hydatid Cyst

Hydatid disease is uncommon in children in nonendemic regions, which is an infestation by *Echinococcus Granulosus* and rarely by *Multilocularis*. Approximately 10-25% of patients present in childhood. The most common sites are the liver (64%), followed by the lung (28%). Pathologically, the cyst has three walls: rigid outer layer formed by modified host cells and liver tissue ; middle laminated acellular membranes ; and inner germinal layer which is known as proliferative cellular membranes. Patients may be asymptomatic or present with discomfort, abdominal swelling without tenderness, or anaphylactic reaction due to rupture. Appearance of a hydatid cyst

changes according to the maturity of the lesions. Provided sonographic features, a hydatid cyst can be classified by Gharbi and WHO classification systems.

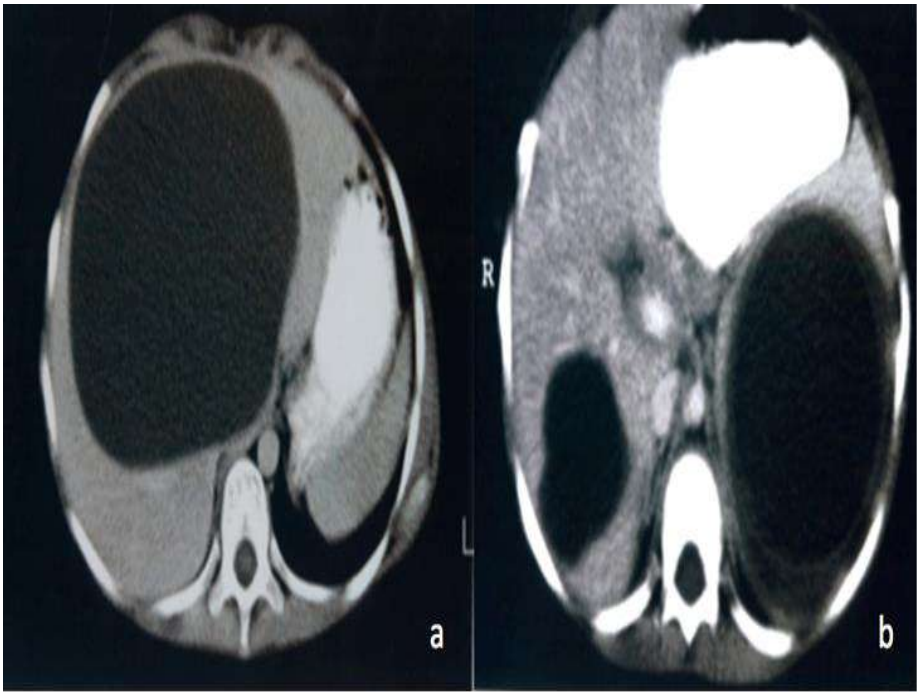

Figure 2: Hepatic hydatid cyst: In two different cases, a unilocular cyst is observed in the liver center (figure a) and the right lobe (figure b).

On US, we may see a well-defined thick-walled univesicular anechoic cyst. Due to detached germinatif membranes, internal septations may be seen. Intracystic debris formation in the dependant part of the cyst may be seen because of hydatid sand. On CT, we location, expendation, and connection of the biliary system, and also wall calcification may be seen.

Detached laminar membranes within the cyst may be seen as hyperdense. Cyst wall and septations may enhance. On MRI, a hydatid cyst is evaluated hypointense on T1W and hyperintense on T2W images. The cyst wall is seen as a hypointense thick rim on T2W images that reflects the collagen-rich outer layer. On treatment, although surgery is mostly the preferred treatment, percutaneous catheter drainage with adjuvant antihelmintic chemotherapy has been performed successfully.

1.3. Choledochal Cysts (CCs)

CCs are congenital cystic malformations of the biliary tree which are primarily seen in children, particularly in the Asian population. It is pancreaticobiliary junction anomalies causes reflux of pancreatic enzymes into the biliary tree, and cystic anomalies occur as a result. Patients frequently present in the first decades of life with typical clinical findings as episodic abdominal pain, cholestatic jaundice, and right upper quadrant masses.

It is known that CCs are associated with biliary atresia with a 44% rate, and also 8-11% of patients with biliary atresia have CCs. Congenital biliary cysts are classified by Todani classification according to the dilated part of the biliary system and the type of cystic dilatation. Type 1 is mostly common, followed by type 4.

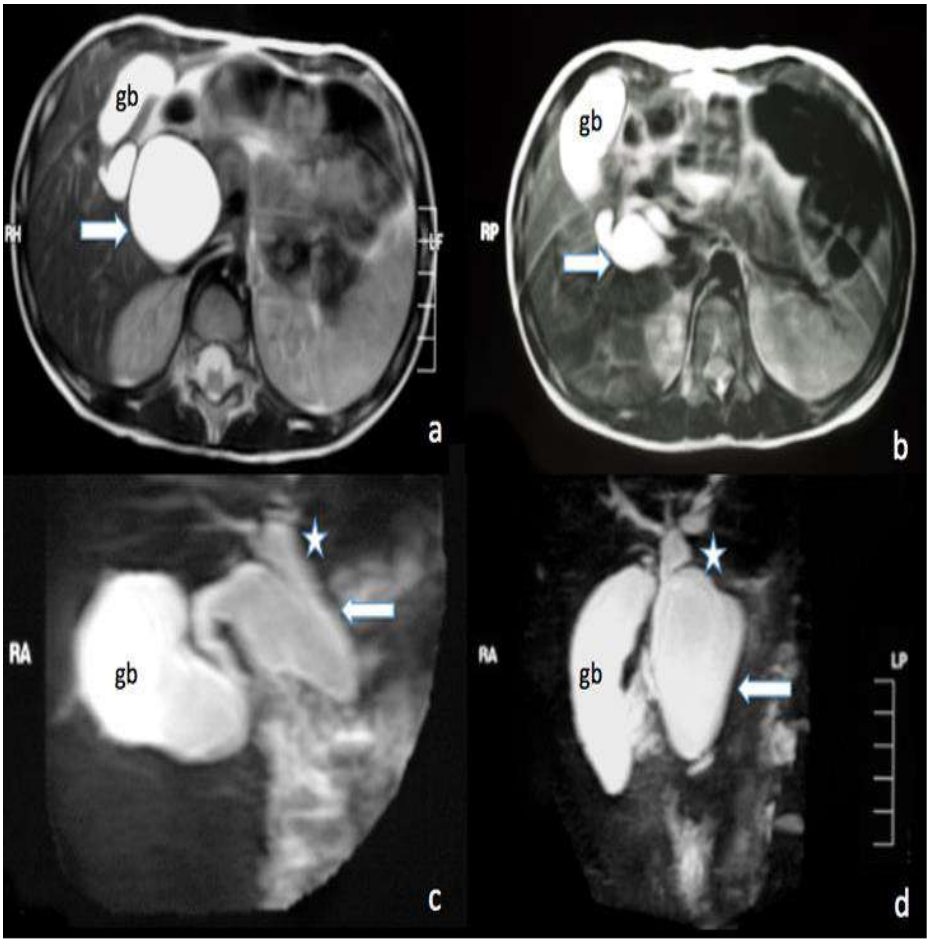

Figure 3: Various choledochal cysts are seen on axial T2-weighted MRI (figure a, b) and MRCP (c, d). Todani Type 1a (figure a), Todani Type 1b (figure b), Todani Type IV (figure c, d) choledochal cyst.

On US, CCs are seen as anechoic simple cysts at common biliary ducts, periportal or peripancreatic area separated from the gallbladder. Biliary origin and communication with biliary ducts can be confirmed by magnetic resonance cholangiopancreatography (MRCP). MRCP may help in classification also. Provided that CCs can be associated with

severe complications such as cholangitis, perforation, liver failure, and malignancy, surgical excision is the mainstay treatment when possible.

1.4. Pancreatic Pseudocyst

Pancreatic pseudocyst is the most common cystic mass of pancreatic tissue in childhood (75%), which occurs either 4-6 weeks after acute pancreatitis or secondary to trauma, mostly this is formed as a result of single or repeated episodes of pancreatitis with a common location of the body or tail part. A pancreatic pseudocyst is a collection of pancreatic fluid (enzymes) and inflammatory exudates encapsulated by fibrous tissue. This finding distinguishes pseudocyst from a true pancreatic cyst. Patients present with abdominal pain, jaundice, nausea, vomiting, anorexia, weight loss, fever, and tender epigastric mass. On US, a well-defined hypoechoic mass (mostly multilocular) with internal septations are revealed.

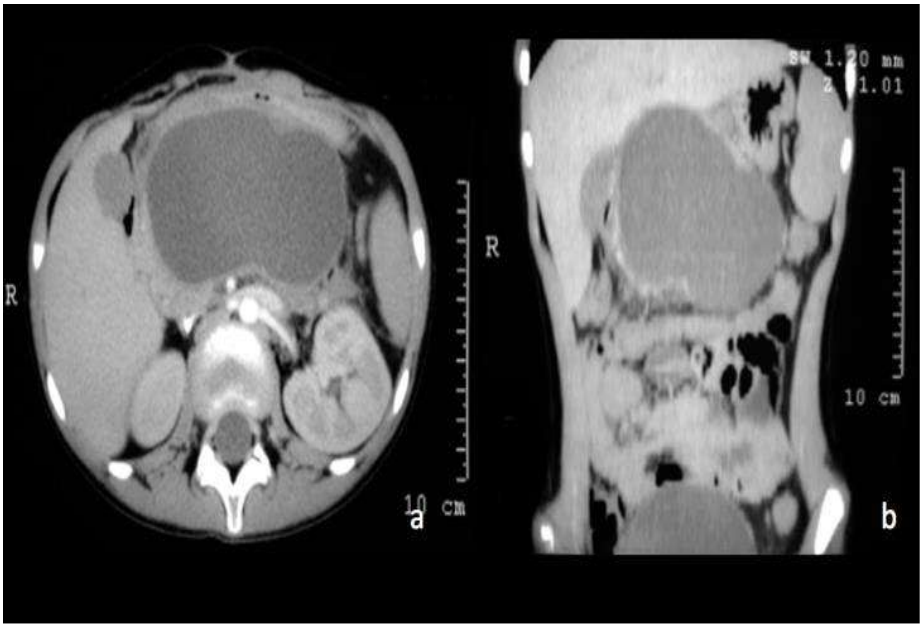

Figure 4: Pancreatic pseudocyst. A unilocular, thin-walled cystic lesion is seen in the pancreatic body in a patient presenting with abdominal pain in the late post-traumatic period.

Internal echoes and fluid-fluid level may be seen in the case of hemorrhage or infection. CT or MRI may be preferred for both treatment and surgical planning. On CT, pancreatic pseudocyst is seen as a round or oval hypodense lesion with low attenuation if it is not complicated. The cyst's effects on adjacent structures may be revealed on US, but CT is better to detect location and contiguous anatomic relations. On treatment, internal or external drainage of the cyst is preferred. Recently, US or CT guided needle aspiration and drainage are used successfully.

1.5. Pancreatic Hydatid Cyst

Pancreatic hydatid disease is rare; it takes up only 1% of all sites of hydatid disease. Because of the other more common cystic disease of pancreatic tissue, diagnosis may be difficult and misinterpreted or delayed. Primary pancreatic hydatid cyst in childhood is extremely rare: there are only five pediatric cases have been reported yet. It is thought that pancreatic infestation is provided by hematogenous spreading rather than local spread by the pancreatic or bile duct. Clinical findings change due to the anatomic localization of the cyst: pancreatic head localization causes jaundice according to compression of the common bile duct, besides pancreatic tail localization causes portal hypertension.

Main clinical symptoms are unexplained epigastric abdominal pain (may be with tender), discomfort, and vomiting.

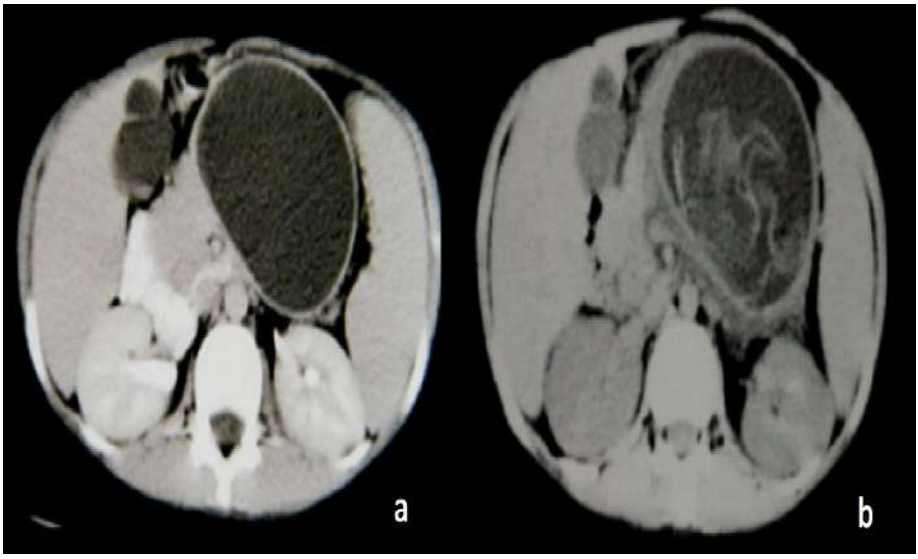

Figure 5: Pancreatic hydatid cyst: Gharbi Type II hydatid cyst with a detached germinative membrane located in the pancreatic body-tail is seen (Figure b).,

On US, we may demonstrate a typical cyst with a various thickened wall. On CT, round or oval cystic lesion with curvilinear calcifications may be seen. Only radiological examinations are insufficient to diagnose pancreatic hydatid disease. The current definitive diagnosis is only made by surgery, and so, laparotomy plays the main role in both diagnosis and cure by multiple procedures such as proper evacuation, pericystectomy and omentoplasty, and distal pancreatectomy (for tail localized cyst).

1.6. Hydrops of the Gallbladder

Noncalculous distension of the bile duct and bile duct hydrops, known as inflammation, is a rare cause of right upper quadrant mass relative to bile stones in hemolytic anemia or idiopathic bile duct pathology in pediatric patients. This entity is often seen in the late stages of adolescence. It is thought that this disease develops due to temporary obstruction associated with cholestasis due to ductal system obstruction causing bile accumulation. Hydrops of the gallbladder may be isolated form or related to upper respiratory infections, Kawasaki syndrome, gastroenteritis, and scarlet fever. Patients present with a palpable mass. On US, a markedly distended gallbladder with normal wall thickness and anechoic contents are evaluated. Bile sludge may be seen. There are neither pericholecystic fluid nor wall thickening and stones seen. The bile ducts appear normal also. On treatment, spontaneous resolution is seen in mostly cases so, surgery is frequently not necessary that US follow-up is sufficient technique for this condition.

2. SPLEEN

2.1. Splenic Epidermoid Cyst

Splenic epidermoid cyst is a rare condition characterized by a congenital nonparasitic true cyst with a 10% rate of all nonparasitic cystic disease of the spleen. The presence of epithelial lining on the wall distinguishes the epidermoid cyst from the pseudocyst. Splenic cysts are supposed to arise from mesothelial inclusion of visceral peritoneum during fetal spleen development, and undergo squamous metaplasia later in life. Splenic cysts are classified in two forms: true cyst and

pseudocyst. Pseudocysts such as epidermoid, echinococcal, and etc. are more common than true ones (pseudocyst is 75%, true cyst 25%). Although congenital epidermoid splenic cysts are seen mostly in adults, the 2nd or 3rd decades of life, they are seen in the pediatric population with a 2.5% rate also. Patients may be asymptomatic or may present with left upper quadrant pain, anorexia, nausea, vomiting, weight loss, diarrhea, fullness, and urinary complaints. These symptoms are usually associated with the displacement and compression effect of the cyst, especially in large ones.

Figure 6: Splenic epidermoid cyst: A thin-walled, large unilocular cystic lesion is observed in the splenic parenchyma filling the left quadrant of the abdomen.

On US, the cyst is anechoic and well defined and sharply demarcated from the surrounding normal splenic tissue. Some cysts may include echogenic fat droplets which give a hypoechoic appearance rather than anechoic. Emergency complications of these cysts are rare (3%) as hemorrhage, rupture, and secondary infection. On treatment, a less than 5 cm cyst should not be operated on but should be followed by US twice a year until complete resolution. Neonatal cysts, when they grow over 5 cm, should be operated on due to their risk of complication (superimposed infection, intracystic hemorrhage, rupture).

2.2. Splenic Pseudocyst

Splenic cysts are classified as true (primary) and pseudocyst (secondary) according to the epithelial lining entity. Pseudocyst is a lack of epithelial lining, so they are called as false cyst. Pseudocyst is presumed to posttraumatic origin as nonresorption of hematoma and splenic infarction. This disease is a 75% rate of all splenic cysts with male predominance. Some authors presume that large posttraumatic pseudocysts are lacking epithelial lining congenital cysts after organized intracystic hemorrhage due to repeated minor trauma. Patients may be asymptomatic or present with epigastric fullness, palpable abdominal mass, pain, and complications due to adjacent organs compression such as urinary obstruction, hypertension with renal artery compression, intracystic hemorrhage, rupture, and etc.. Sonography or CT reveal the splenic origin of the lesion on its cystic nature.

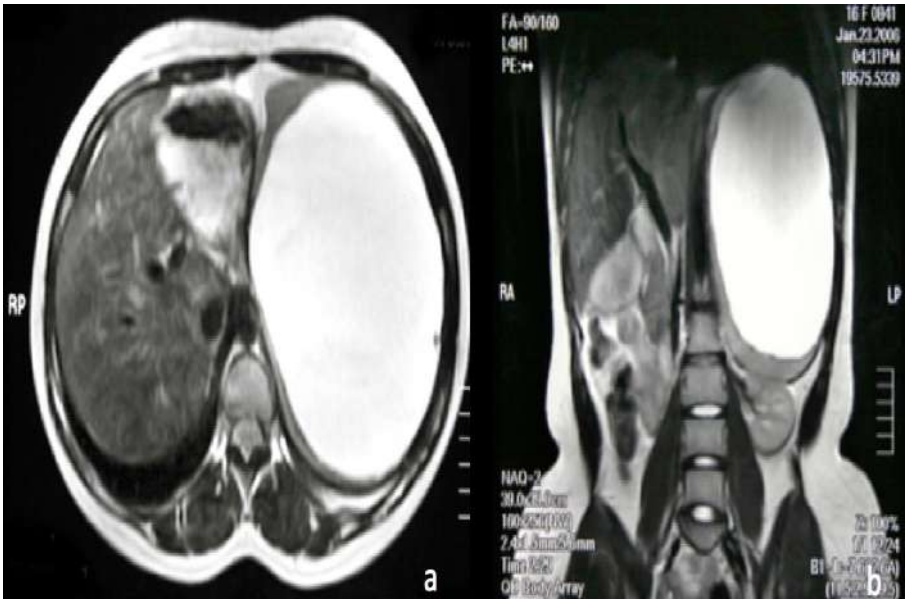

Figure 7: Splenic pseudocyst. A large unilocular cystic lesion with thin walls is observed in the splenic parenchyma.

On US, both congenital (true, epidermoid) and pseudocysts are seen as unilocular anechoic round lesions with acoustic enhancement. While pseudocysts often have thicker walls (maybe calcified), a congenital cyst's wall is vaguely. If it contains debris or hemorrhage, we may see internal echoes, layering fluid-fluid level within the cyst (the dependent layer is more echogenic).

On CT, there is no internal enhancement additionally. CT is preferable in detected calcification, trabeculation, or septation on the cyst wall. On treatment, likely epidermoid cyst, a less than 5 cm cyst should not be operated on.

3. KIDNEYS

3.1. Multilocular Cystic Nephroma

Multilocular cystic nephromas are rare nonhereditary benign cystic renal neoplasms which are ranging from cystic nephroma (lined by epithelium and fibrous septa with mature tubules) and cystic partially differantiated nephroblastoma arises from maldevelopment of the ureteral bud. Multilocular cystic nephromas have male predominance typically occur in between 3 months and 2 years old. Patients present with palpable abdominal mass without pain. Hypertension and hematuria may be seen also. On US, well circumscribed, multiloculated, encapsulated anechoic multicystic mass with internal echogenic septation is seen. There is no communication among cysts. It may range in size from a few centimetres (cm) to 10 cm. Cyst may extend through the renal capsule. CT is not necessary after from US, incidentally detected multilocular cystic nephroma may be while CT examined for other conditions. On CT, well circumscribed multiseptated with thickness, and enhancement mass may be seen. Although calcification is rarely, it may be seen on CT also. On treatment, since imaging studies are insufficient to distinguish multilocular cystic nephroma from multilocular cystic renal cell carcinoma or cystic Willms tumor, nefrectomy is preferable choice.

3.2. Multicystic Dysplastic Kidney (MCDK)

MCDK is a unilateral acquired developmental renal dysplasia which is the most common neonatal mass of kidney. Early in utero urinary tract obstruction causes pyeloinfundibular atresia result in MCDK.

Diagnosis is frequently made in fetal life with detection multiple discommunicated cysts without central large cyst. While autosomal dominant polycystic kidney disease, which is the most common hereditary cystic disease involving both kidneys, MCDK is seen always unilaterally.

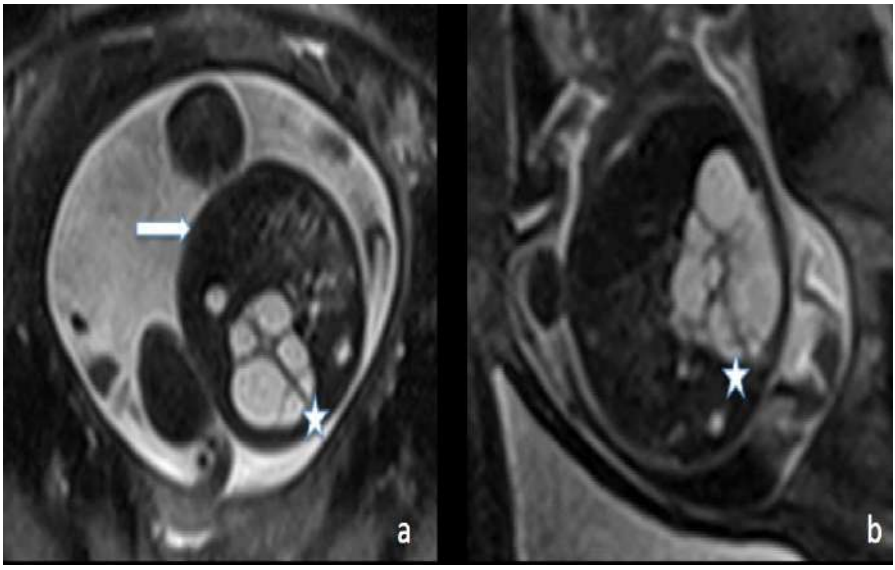

Figure 8: Multicystic Dysplastic Kidney: In the fat-suppressed axial T2-weighted imaging of the fetal MRI, the parenchymal tissue of the fetal right kidney is not observed, and multiple cystic lesions are seen in this area.

On US, multiple anechoic cysts and missing parenchymal tissue may be seen. Contralaterally renal abnormally such as vesicoureteral reflux, ureteropelvic junction obstruction and primary megaureter may be seen about 20-50% of patients so it is important to bilateral renal examination adding. On MRI, MCDK' cystic lesions are hypointense on T1W and hyperintense on T2W imaging if they are

not complicated. MRI urography and coronal images are useful to reveal the noncommunication among cysts and non-dilatation on renal pelvis in MCDK, so that we may discriminate between MCDK and hydronephrosis. Renal scintigraphy confirm the diagnosis by revealing absence of functioning tissue with no radiotracer uptake. On treatment, since hypertension and malignant degeneration (Willms or renal cell ca) are experienced rarely, uncomplicated MCDK may be followed by US.

3.3. Renal Hydatid Cyst

Hydatid disease of kidney in childhood is quite rare even in the endemic areas and constitutes 2-4% of all hydatid disease, although renal involvement is the third most common localization after the liver and lung respectively. By the way renal hydatosis may appear together with other organs involvement, only renal cyst is extremely rare. Infestation by passing through the portal system into the liver and retroperitoneal lymphaticis or directly via the gastrointestinal tract may be accused for etiology. Patients are mostly asymptomatic or present with flank pain, hematuria, and anaphylactic reaction in case of rupturation. Mass effect to adjacent structures may be seen if there is a large size identification. US is the most sensitively technique for detection the stage and also useful to follow up.

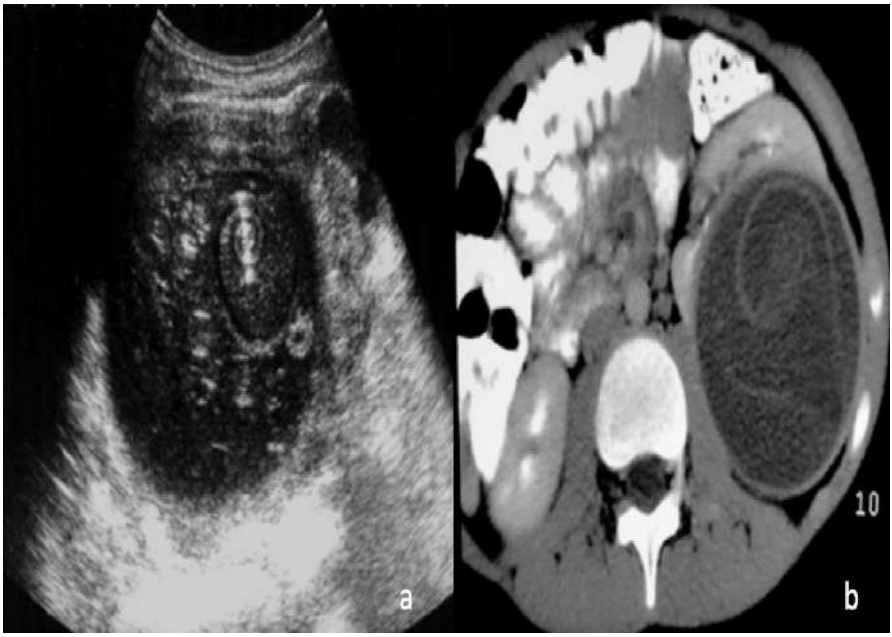

Figure 9: Renal hydatid cyst: USG (figure a) and CT examination (figure b) show a Gharbi type II hydatid cyst with a detached germinative membrane in the left kidney.

On US, we may see well circumscribed, unilocular, anechoic lesion with posterior acoustic enhancement. Solid content of the cyst, called as hydatid sand, is seen likely punctate echogenicity inner the cyst. On CT, well defined, round or oval masses with lower density and liquid content without contrast enhancement may be seen. In case of entity, calcification may be detected on CT also.

On treatment, medicine (antihelminticis) is a choice for uncomplicated cyst, but if there is an over than 7 cm size of cyst, conventional surgery is necessary due to rupture the other complications risk.

3.4. Urinoma

Urinoma is a rare complication of childhood described as an encapsulated urine extravasated collection which is originated from secondary congenital obstructive uropathies mostly posterior uretral valve, or acquired reasons such as calculous, retroperitoneal fibrosis, malignancy of renal pelvis, ureter or bladder. Nonobstructive reasons include kidney or collecting system trauma. Spontaneous urinoma is extremely rare. As mechanism urine extravasation into the retroperitoneum causes lipolysis of adjacent fat tissue, and as a result, encapsulation of urine called urinoma. Extravasated urine may be intraperitoneally, extraperitoneally or in both locations. Intraperitoneal location is the most common presentation. There are 4 type described: localized perirenal (most common), diffuse perirenal, subcapsular, and intrarenal.

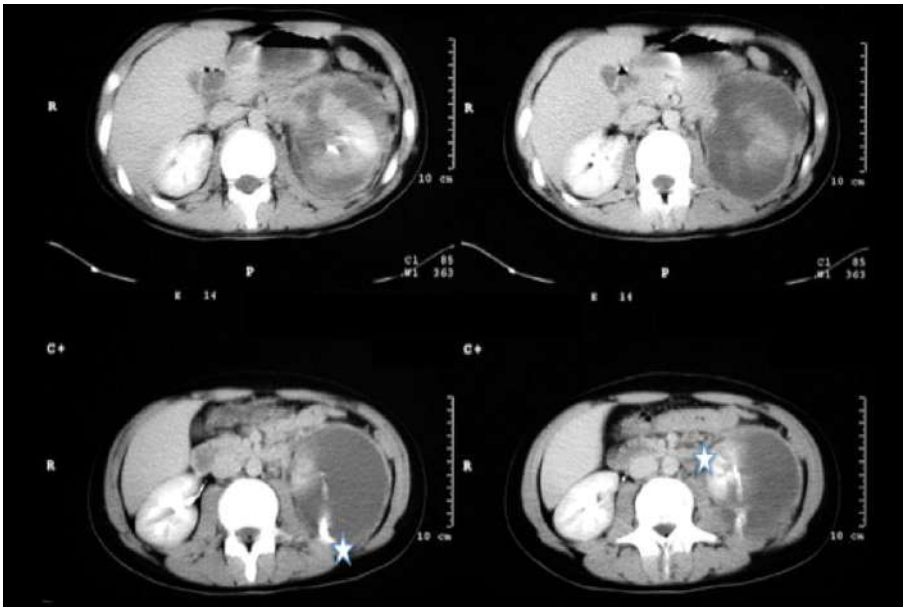

Figure 10: Urinoma: In the case where a cystic lesion was detected in the left kidney after trauma, a retroperitoneal cystic lesion accompanied by contrast material leakage associated with the parenchyma (figure c, d star) is observed in the CT sections taken during the left pyelogram phase.

On US, thinned walled anechoic well circumscribed collection with partially containing any portion of renal tracts may be seen. On CT and MRI, urinoma shows water attenuation, hypointensity on T1W and hyperintensity on T2W images. On late phase (excretory phase) contrast enhanced imaging may show the urine leakage as direct contrast extravasation from urinary tract. On treatment, small urinomas are frequently approached conservatively, larger, persistent or symptomatic ones usually need to percutaneous drainage due to urine leakage.

4. BOWEL AND MESENTERY

4.1. Lymphangioma

Mesenteric lymphatic malformation known as mesenteric/omental cysts are cystic lymphangiomas of small bowel mesentery and omentum respectively. This condition arises from secondary to congenital malformation of abdominal and/or retroperitoneal lymphatics with lack of communication beyond the lymphatic system. Lymphangiomas mostly occur in the neck and axillary region (95%), in the abdomen, the most common location is mesentery followed by omentum, mesocolon and retroperitoneum. Patients present with

abdominal pain (80%), distention, mass, nausea, vomiting, weight loss, fever, peritonitis, and etc. Further complications are hemorrhage, rupture, and torsion leading to volvulus.

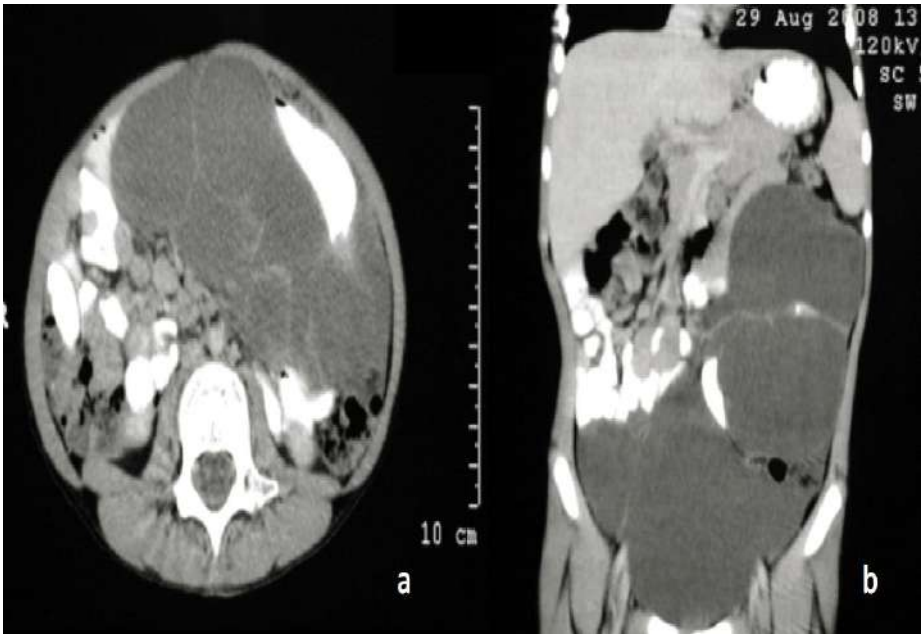

Figure 11: Lymphangioma: A multiloculated septate cystic lesion filling the left upper and lower quadrants of the abdomen is observed.

On US, lymphangiomas appear as sharply defined, mostly multiloculated, round anechoic masses, frequently with septation. If it is complicated with hemorrhage or infection, debris may be seen as hyperechogenicity within the cyst. On CT, thin walled, uni-multiloculated round or oval cystic masses with low density (range from water to fat) and septal enhancement may be seen. Also, calcification may be seen with rarity in pediatric patients rather than adults. Large lymphangiomas are confused with severe ascites.

Separation of bowel loops, fluid collection in perihepatic and douglas spaces, lack of septation may be helpful to determine the ascites and distinguished from the lymphangiomas.

On MRI, the contents may be hypointense on T1W and hyperintense on T2W, or hyperintense on both T1W and T2W images. On treatment, complete surgical excision with possible bowel resection is preferred if the lesion is intimately attached to bowel.

4.2. Enteric Duplication Cysts

Enteric duplication cyst is a rare focal congenital cystic anomaly of gastrointestinal tract which occur anywhere along the mesenteric border of the bowel but most commonly in jejunum or ileum. Etiologically, malrecanalization of solid part of fetal intestines and its separation from neuroenteric canal and ischemia to the intestine is blamed for this disease. Duplication cyst lined with inner intestinal epithelium, and there is smooth wall muscle within its wall.

Although most cysts are closed cystic duplication without communication with bowel, rarely association with bowel may be seen. This finding is an important image for duplication cyst and is used to distinguish it from mesenteric cyst.

Patients are within the first year of life and mostly asymptomatic or present with palpable abdominal mass, distention, vomiting (due to bowel obstruction), or hemorrhage (due to peptic ulceration presence of gastric mucosa).

Figure 12: Enteric duplication cyst: Bilobed large cystic lesion is observed on standing direct abdominal radiography (ADBG) (Figure a) and coronal T2-weighted MRI.

On US, cyst is ovoid, spheric or dumbbell shape, well circumscribed, with characteristic bowel wall features, called as ‘rim sign’ or ‘gut signature’ that includes echogenic inner rim of mucosa and hypoechogenic outer rim of muscle layer, frequently detected in dependent side of the cyst. Cystic content may be anechoic if it is not complicated. Some cyst may contains internal echoes and septation due to hemorrhage or mucoid material. On CT, a well defined round masses with water attenuation and mildly wall enhancement are seen. On MRI, duplication cysts are hypointense on T1W, and hyperintense on T2W images. Hemorrhagic and mucoid content may present hyperintense

features on T1W images. On treatment, current approach in symptomatic patients is surgical excision while there is no standardized evidence based guidelines on management for incidentally detected asymptomatic patients.

4.3. Intraperitoneal Hydatid Cyst

Hydatid diseases are seen 64% in the liver, 28% in the lung, and 8% in other anatomic localizations. Peritoneal hydatidosis is a rare condition even in the endemic areas. Peritoneal hydatid disease may be primarily or more commonly secondary to hydatid cyst in the liver followed by the spleen. Primarily peritoneal hydatidosis is extremely rare with no sufficient mechanism. It is believe that dissemination via lymphatics or systemic circulation may causes peritoneal infestation. Secondary forms almost always originate from hepatic hydatid disease by surgical or spontaneous rupture. Patients may be asymptomatic or present with insignificant symptoms such as abdominal pain and swelling.

On US, we may see unilocular well defined thick walled hypo-anechoic cystic lesions and septa and hydatid sand as usual. On CT, wall calcification and septation may be detected also. On MRI, we may demonstrate the cyst wall defect in case of entity additionally. On treatment, curative or palliative surgical treatment is preferred management, while medical one (antihelmintic) is effective alternative for small and asymptomatic cyst.

5. PELVIC CAVITY

5.1. Hematocolpos / Hematometrocolpos

Hematocolpos/hematometrocolpos is characterized by a fluid-filled dilated vaginal and uterine cavities due to distal vaginal outflow obstruction. Imperforate hymen, vaginal atresia-agenesia, cervical stenosis are the most common causes of obstruction. Patients frequently present with pelvic midline mass (80%), abdominal distention, urinary obstruction and etc. Amenorrhoea and cyclic pelvic pain are seen in adults.

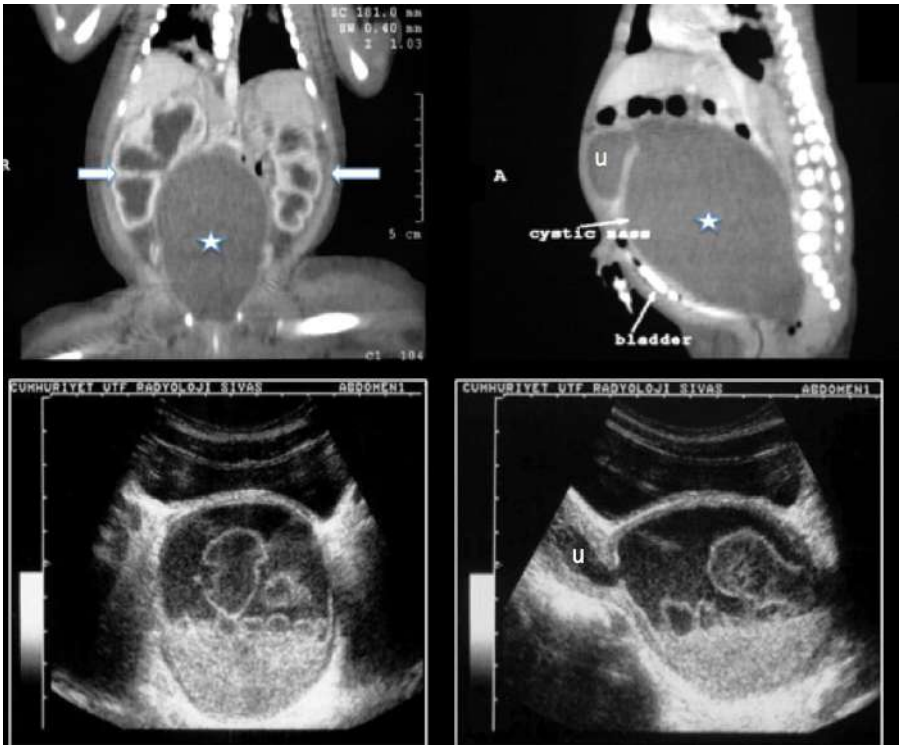

Figure 13: Hematometrocolpos: Vaginal atresia is detected in a patient evaluated for abdominal pain and distension. Coronal and sagittal CT scans reveal extensive cystic dilatation of the cervix and

uterus, which compresses the bladder and both ureters, leading to hydronephrosis. Ultrasonography reveals the leveling of debris from the cystic dilatation.

On US, large, spherical or round cystic pelvic midline mass with internal echoes are seen which point to mucoid and cellular debris. Fluid-debris level may be shown on US also. On CT, well circumscribed, hypodense cystic lesion with fluid-debris or fluid-hematocrit level is demonstrated. On MRI, protein rich or hemorrhagic content is seen as hyperintense on T1W images. On treatment, if etiological reasons are cleared away, patients recovery very well.

5.2. Mature Cystic Teratoma (MCT)

MCT which is composed of tissue from at least two or three germ layers (endoderm, mesoderm, ectoderm) is the most common benign adnexial lesion in children. The most common localization is sacrococcygeal area (47,2%) followed by gonad (31,6%) with female predominance. It rarely occurs on extragonadal site. Patients present with large midline abdominal mass without pain. If it is torsioned (15%), tenderness and pain may be seen also. Additionally, presacral tumor may be completely internal, so it occurs with obstructive and compressive symptoms on adjacent structures. Plain films show calcification resembling tooth.

On US, hypoechoic cystic mass, hypo-hyperechoic solid component may be seen. Also we may see calcifications with posterior acoustic shadow arising from the ectodermal part. A Rokitansky nodule

implies a solid mass attached to the wall of cyst including teeth, fat, hair or bone. On CT, fat attenuation content, calcification and teeth may be determined. On MRI, T1W and T1W signal changes according to the solid component of lesion: fat is seen hyperintense both T1W and T2W images, while calcification is seen as signal void in both. Solid component may shows contrast enhancement also. In sacrococcygeal teratoma, MRI is preferable technique to reveal the intraspinal extension of the mass as a clue to its origin. On treatment, although cystic tumors have better prognosis than solid ones, surgical treatment is necessary for these lesions due to the risk of malignancy.

5.3. Ovarian Cysts

Ovarian cyst is the most common ovarian mass found in newborn. They are classified in three groups: physiological, functional and neoplastic. Physiological cysts are normal follicle cyst and corpus luteum with 80% of all primary ovarian masses and they are frequently less than 3 cm. Meanwhile in the first 3 months of life, small follicular cyst may be seen due to placental and maternal hormones transition. Functional cysts are originated from failed involution of the follicle or corpus luteum account for one-fourth of primary ovarian lesions. They frequently present with intracystic hemorrhage. Neoplastic cysts are the one-half of all primary ovarian lesions and the most common presented type is mature cystic teratoma followed by serous and mucinous cystadenoma. Patients are asymptomatic or present with lower abdominal pain, distention, and in case of torsioned, hemorrhage with acute abdominal pain may be seen also. On US, well defined, thin

walled, anechoic cystic lesion with posterior acoustic enhancement may be seen. Detecting the surrounding normal ovarian tissue or a 'daughter cyst' along the cyst wall is 100% specific and 82% sensitive features for ovarian cyst. Hemorrhagic ovarian cyst shows fluid-debris level, septation or solid-like appearance. It is important to distinguish hemorrhagic cyst from cystic ovarian neoplasm, so absence of vascularity for hemorrhagic cyst on Color Flow Doppler useful feature for discription. On CT, ovarian cysts are well defined hypodense with enhancement at cyst wall, septations and surrounding normal ovarian tissue. On MRI, cysts appear hypointense on T1W and hyperintense on T2W images. Hemorrhagic cyst may be hyperintense on T1W and low signal on T2W images. Mature cystic teratomas contain calcification, fat or hair. They are thin walled cystic mass with multiple septation and intermixed solid areas.

Mural nodules and echogenic foci with acoustic shadow may be seen. We have mentioned about mature cystic teratoma previously. Serous and mucinous cystadenomas are rare in children, usually in postpubertal period.

Cysts are large (more than 20 cm in diameter) and papillary processes may be seen along the wall. On treatment, uncomplicated cysts less than 4 cm in diameter should be followed up by US, because they are usually show spontaneous regression (25-50%). Large or complicated cysts should be treated surgically. If there is malignancy suspicion, surgery is necessary also.

5.4. Pelvic Hydatid Cyst

Hydatid disease are seen most commonly in the liver (64%) followed by lung (28%), kidney (3%), bone (1-4%) and brain (1-2%) respectively, although infestation may be seen in every site of body such as spleen, muscle, heart, pancreas, omentum, ovaries, parametrium, thyroid, orbit, retroperitoneum, pelvis and etc.. Pelvic hydatid disease is frequently secondary to spontaneous or acquired rupture (in surgery or trauma) of primary hydatid cyst (most commonly from liver followed by spleen). Primary pelvic hydatid cyst is extremely rare (2,2%) and most accepted reasons is dissemination of hydatid embryo via hematogenous or lymphatic circulation. Patients frequently present with non-specific mass with compression effect on adjacent organs such as urinary bladder or rectum and rarely it may cause obstructive uropathy and renal failure. US and CT may help to reveal the location, to characterize the nature such as size, calcification, density, hydatid membranes, relation with adjacent structures. On treatment, antihelminticis are successful approach while surgery is most effective management. Combination of preoperative antihelmintic, surgery and postoperative antihelminticis procedure is the most successful regime.

5.5. Abdominoscrotal Hydrocele (ASH)

ASH is a rare anomaly comprising between 0,4-3,1% of pancreatic hydrocele. Most patients are younger than 1 year with a fluid-filled mass which has inguinoscrotal and abdominal components. Etiology of ASH is not well known yet but the mostly accepted theory is expansion

over time of a large scrotal hydrocele across the internal inguinal ring into the extraperitoneal space due to partial obliteration of processus vaginalis. Patients are asymptomatic or present with mass and compression effects on adjacent structure in larger sizes. Diagnosis is frequently made by physical examination that large tense hydrocele and abdominal mass which are cross fluctuant is seen.

Figure 14: Abdominoscrotal hydrocele. Coronal T2-weighted imaging shows an hourglass-shaped cystic lesion extending from the scrotum to the intra-abdominal space.

On US, thin walled cysts with compartments, rarely a single cyst may be seen. Cyst may contain fluid or fat but not solid parts. On CT and MRI, enhanced cyst wall and septation (if it is) may be seen additionally. On coronal images 'hour glass sign' may be determined also. In literaturely, malignant degeneration into paratesticular malignant mesothelioma is described only once. On treatment, early surgery is preferred due to the rarity of spontaneous resolution and the probability resulting in hydronephrosis.

5.6. Megacystis

At first trimester fetal megacystis are seen approximately 1:1500 pregnancies with male predominance (8:1). The underlying causes are in two types: obstructive and nonobstructive conditions. Obstructive conditions are most commonly in male characterized by maldevelopment of urethra such as PUV, while the female bladder obstruction is frequently result of more complex defects in development of urogenital system as cloacal plate abnormalities. US detects the dimension of the fetal bladder from 10 weeks of gestation. Diagnostic dimension changes accoring to gestational age ; bladder longitudinal diameter in the 1st trimester: greater than or equal to 7mm ; bladder longitudinal diameter in the 2st trimester: greater than or equal to 30mm ; bladder longitudinal diameter in the 3st trimester: greater than or equal to 60 mm. But generally accepted opinion that in first trimester bladder longitudinal diameter of > 7mm, later in pregnancy, a sagittal dimension (in mm) greater than gestational age (in weeks). Megacystis may be found in several conditions such as posterior urethral valves

(PUV), Prune Belly Syndrome (PBS), urethral atresia or stenosis, cloacal abnormalities and megacystis-microcolon-intestinal-hypoperistalsis syndrome.

Figure 15: Megacystis. Cystic dilatation of the bladder is observed on fetal MRI.

On US, enlarged bladder with thickened, (more than 3mm) trabeculated wall and 'key hole sign' may be seen. Key hole sign is important discriminating feature between PUV and PBS. Sometimes renal hyperechogenicity may be seen and it is a clue of poor prognosis. Paravesical arteries are important sign to distinguishes true bladder from other cystic structure within the pelvis. Oligohydroamnios are seen in half of cases with poor prognosis. > 17 mm bladder length and chromosomal abnormality (20%), particularly trizomi 13 and 18 are poor prognostic factors, too. On treatment, mild first trimester megacystis (over than 15 mm in diameter) show spontaneous resolution, so US follow up may be preferred.

Persistent megacystis prognosis is poor for fetus and termination is usually advised. It is important to assess gestational age, sex and any associated sign to discriminate between the obstructive and nonobstructive causes.

5.7. Resolving Adrenal Hemorrhage

Adrenal hemorrhage, which generally occurs in infants is frequently result from neonatal sepsis, hypoxia, birth trauma, coagulopathia, hypotension, and etc.. While the right adrenal gland is the most effected side, left adrenal gland hemorrhage is associated with renal vein thrombosis. Patients present with palpable mass, anemia, and jaundice due to hyperbilirubinemia. Imaging findings change according to stage of hemorrhage.

On US, acute adrenal hemorrhage is seen as a suprarenal cystic mass with variable echogenicity and complexity. Subacute hemorrhage becomes more hypoechogenic due to clot retraction and calcification.

On CT, acute adrenal hemorrhage is in 50-90 HU density and decreases on follow up within days to weeks. Lately stage, calcification and resolving may be seen obviously on CT. On MRI, signals change according to age of blood products. Acute hemorrhage is intermediate or hyperintense on T1W images.

Chronic hematoma is hypointense on T1W and hyperintense on T2W or hypointense on T1W and T2W images.

On treatment, follow up US may help to document the resolution of hematoma and to discriminate between adrenal hemorrhage and neuroblastoma, which are both similar on imaging. Provided the follow up, while adrenal hemorrhage decreases in size within 1-2 weeks, neuroblastoma remains stable or increase in size.

5.8. Tailgut Cyst

Tailgut cysts, known as retrorectal cystic hamartoma, is a rare congenital anomaly which occur as a retrorectal or presacral multilocular cystic mass lined with gastrointestinal type of epithelium found in infancy or persisting undetected into adulthood.

It is suggested that this lesion arises from persistence of embryonic hindgut. Patients are asymptomatic or present with abdominal pain or constipation.

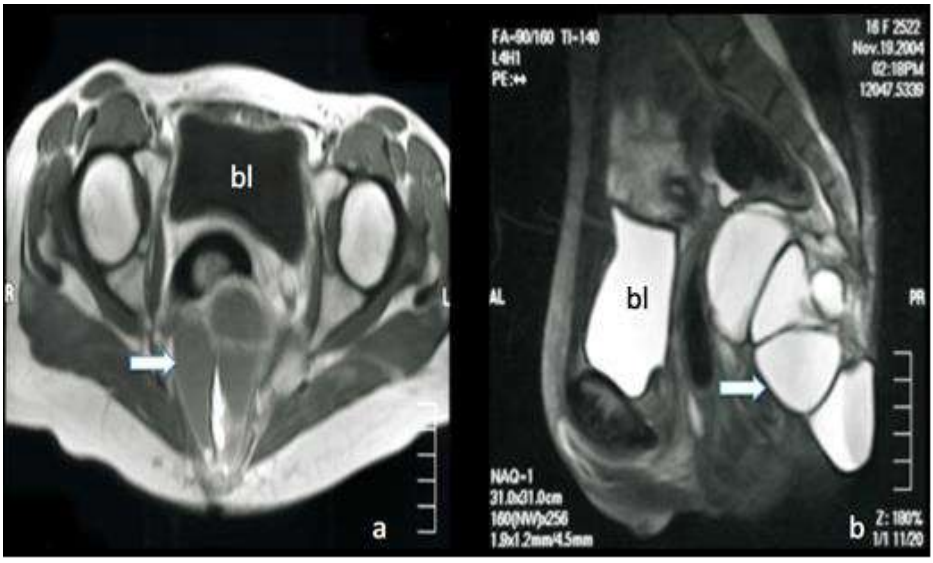

Figure 16: Tailgut cyst: A multiloculated cystic lesion is observed in the presacral distance in axial T1-weighted (figure a) and sagittal T2-weighted (figure b) images.

On US, well defined, multilocular, retrorectal cystic mass is seen. Multicystic nature of the mass and presence of keratinous material or inflammatory debris cause internal echoes within low level of mass. On CT, well circumscribed with water or soft tissue density may be seen. Rarely, calcification is demonstrated into the cyst wall. If infection or malignant transformation occur, breaking down of margins and involvement to adjacent structures may be seen also.

On MRI, tailgut cyst is frequently hypointense on T1W images and hyperintense on T2W images.

Mucinous content, high protein or hemorrhage are seen hyperintense on T1W images.

Irregular wall thickening or polypoid mass with intermediate signal intensity on T1W and T2W together with enhancement are suspicious features for malignancy.

Even if it is difficult to distinguish tailgut cyst from other presacral cysts by imaging modalities, this distinction is very important because of malignancy potential of tailgut cyst. So, pathological examination is definitive diagnosis for tailgut cyst. On treatment, excision is necessary due to malignant transition.

6. MISCELLANEOUS

6.1. CSF Pseudocyst

Peritoneal CSF pseudocyst, known as CSFoma, is a rare complication of ventriculoperitoneal (VP) shunt catheter placement. This complication is seen only with 3% prevelancy and occurs in a ranges from 3 weeks to 5 years after shunting procedure.

Patients present with abdominal pain, distention, mass, and shunt malfunction result in increased intracranial pressure. While larger pseudocyst tend to be sterile, smaller ones are more often infected.

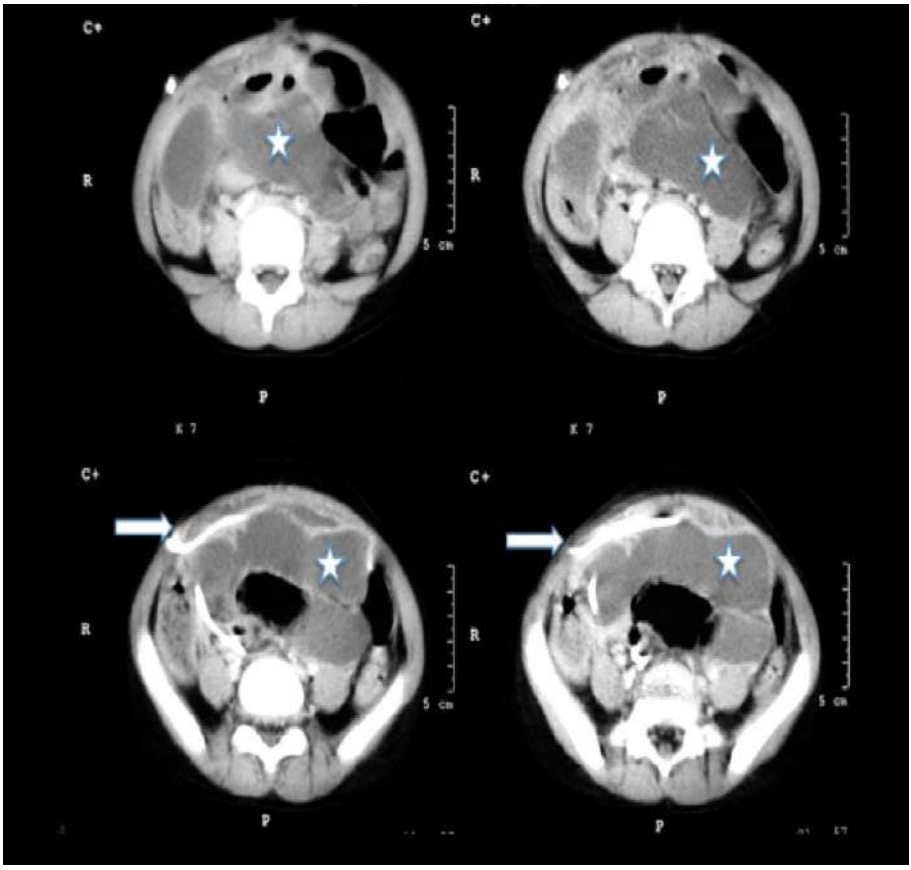

On US, well defined, homogenous anechoic cystic mass located near the tip of VP shunt catheter or maybe catheter tip is identified within the collection. Infected collection shows septations, fluid-fluid level or internal debris also. On CT, loculated cyst like appearance in the peritoneal cavity at the distal tip of VP shunt may be seen. On treatment, shunt revision and aspiration of the cyst should be considered although it mostly shows spontaneous resolution.

6.2. Diaphragmatic Mesothelial Cysts

Diaphragmatic mesothelial cyst lined with mesothelial cells is a rare benign congenital lesion which originate from coelomic remnants. Mesothelial cysts occur in various anatomical sites such as adrenal gland, spleen, ovary, vaginal process of the testicle, falciform ligament and rarely diaphragm. Because of its anatomical relationship with adjacent structures, diaphragmatic cyst may be misdiagnosed with hydatid cyst, simple hepatic cyst and another cystic lesion. Patients are mostly asymptomatic, but chest discomfort, right hypochondriac pain and nonspecific abdominal complaints may be seen. On US, there is a bilobed shape, thin walled, homogenous anechoic cystic lesion in the right posterolateral costophrenic angle, between the thoracic wall and the liver. Bilobulation should be considered diaphragmatic mesothelial cyst and this condition usually associated with complex embryological diaphragmatic development. On CT, well circumscribed, bilobed, homogenous water density cyst may be seen. Rarely, calcification on the cyst wall may be seen. On MRI, thin walled cyst with hypointense on T1W and hyperintense on T2W images may be seen also. On treatment, asymptomatic children can be managed with US follow up. Symptomatic children with large cyst in diameter should be treated with percutaneous sclerotherapy.

6.3. Congenital Pyloric Atresia (CPA)

CPA is a rare congenital anomaly characterized by complete or partially obliteration of gastric lumen. This disease is 1% part of all bowel atresia and found in 1:100 000 births. It is believed that this

anomaly is a result from lack of development on between the 5th and 12th gestational weeks. CPA may occur as an isolated form or associated with other anomalies, mostly epidermolysis bullosa followed by aplasia cutis, duodenal/ileal/colonic atresia and duplication cyst. CPA occurs in 3 types; type 1 is pyloric web or membranes (most presented type), type 2 is pyloric atresia with a solid core of tissue on replacing the pyloric canal, type 3 is pyloric atresia with a gap between stomach and duodenum. Patients present with non bilious vomiting, polyhydramnios, abdominal distention and obstructive and compressive findings. On plain film, dilated stomach with the typical 'single bubble appearance' and no air beyond the pylorus are mainstain features for CPA. Mostly, plain films with clinical findings are sufficient to diagnose, no further images are needed. On US, during prenatal period (especially at first trimester), dilated stomach and gastric outlet narrowing with polyhydramnios may be seen. During postnatal period, US is a complementary technique and stretched-out layered structure of the site of the pylorus with thin mural layers and absence of both echogenic image of the pyloric muscle can be seen. Additionally, US shows that in pyloric atresia, pylorus is seen longer than normally and this feature is important to distinguish this disease from pyloric stenosis which has small and thickened pyloric wall. On treatment, surgical restoration of pyloric atresia is necessary, also duodenoplasty or duodenojejunostomy can be added in case of duodenal atresia association.

7. REFERENCES

- Ranganath, S. H., Lee, E. Y., & Eisenberg, R. L. (2012). Focal cystic abdominal masses in pediatric patients. AJR, 199, W1-W16.
- Wootton-Gorges, S. L., Thomas, K. B., Harned, R. K., Wu, S. R., Stein-Wexler, R., & Strain, J. D. (2005). Giant cystic abdominal masses in children. Pediatr Radiol, 35, 1277-1288.
- Haddad, M. C., Birjawi, G. A., Hemadeh, M. S., Melhem, R. E., & Al-Kutoubi, A. M. (2001). The gamut of abdominal and pelvic cystic masses in children. Eur. Radiol, 11, 148-166.
- Moosavi, S. Y., & Kermany, H. K. (2007). Epigastric mass due to a hydatid cyst of the pancreas: a case report and review of the literature. JOP. J Pancreas, 8(2), 232-234.
- Arıkan, A., Sayan, A., & Erikci, V. S. (1999). Hydatid cyst of the pancreas: a case report with 5 years' follow-up. Pediatr Surg Int, 15, 579-581.
- Brown, R. A., Millar, A. J. W., Steiner, Z., Krige, J. E. J., Burkimsher, D., & Cywes, S. (1995). Hydatid cyst of the pancreas: a case report in a child. Eur J Pediatr Surg, 5, 121-124.
- Onur, M. R., Bakal, U., Kocakoc, E., Tartar, T., & Kazez, A. (2013). Cystic abdominal masses in children: a pictorial essay. Clinical Imaging, 37, 18-27.
- Khong, P. L., Cheung, S. C. W., Leong, L. L. Y., & Ooi, C. G. C. (2003). Ultrasonography of intra-abdominal cystic lesions in the newborn. Clinical Radiology, 58, 449-454.
- Chang, T. S., Ricketts, R., Abramowksy, C. R., Cotter, B. D., Steelman, C. K., Husain, A., & Shehata, B. M. (2011). Mesenteric cystic masses: a series of 21 pediatric caes and review of the literature. Fetal and Pediatric Pathology, 30, 40-44.

• Younger, K. A., & Hall, C. M. (1990). Epidermoid cyst of the spleen: a casae report and review of the literature. British Journal of Radiology, 63, 652-653.

• Dachman, A. H., Ros, P. R., Murari, P. J., Olmsted, W. W., & Lichtenstein, J. E. (1986). Nonparasitic splenic cysts: a report of 52 cases with radiologic-pathologic correlation. AJR, 147, 537-542.

• Touloukian, R. J., & Seashore, J. H. (1987). Partial splenic decapsulation: a simplified operation for splenic pseudocyst. Journal of Pediatric Surgery, 22, 135-137.

• Musy, P. A., Roche, B., Belli, D., Bugmann, P. H., Nussle, D., & Coultre, C. L. (1992). Splenic cysts in pediatric patients: a report on 8 cases and review of the literature. Eur J Pediatr Surg, 2, 137-140.

• Robbins, F. G., Yellin, A. E., Lingua, R. W., Craig, J. R., Turril, F. L., & Mikkelsen, W. P. (1977). Splenic epidermoid cysts. Ann Surg, 3, 231-235.

• Amrani, A., Zerhouni, H., Benabdallah, F. F., Belkacem, R., & Outarahout, O. (2003). Renal hydatid cyst in children: 6 case reports. Annales d'urologie, 37, 8-12.

• Wani, I., Lone, A. M., Hussin, I., Malik, A., Thoker, M., & Wani, K. A. (2010). Peritoneal hydatidosis in a young girl. Ghana Medical Journal, 44, 163-164.

• Yen, J. B., Kong, M. S., & Lin, J. N. (2003). Hepatic mesenchymal hamartoma. J paediatr Child Health, 39, 632-634.

• Moscatelli, G., Moroni, S., Freilij, H., Salgueiro, F., Bournissen, F. G., & Altcheh, J. (2013). Short report: a five-year-old child with renal hydatidosis. Am. J. Trop Med Hyg, 89(3), 554-556.

• Vyas, S., Prakash, M., & Khandelwal, N. (2010). Peritoneal hydatidosis. Postgrad Med J, 86, 255.

• Akıncı, D., Akhan, O., Ozman, M., Ozkan, O. S., & Karcaaltincaba, M. (2004). Diaphragmatic mesothelial cysts in

children: radiologic findings and percutaneous ethanol sclerotherapy. AJR, 185, 873-877.

• Nijs, E., Callahan, M. J., & Taylor, G. A. (2005). Disorders of the pediatric pancreas. Pediatr Radiol, 35, 358-373.

• Rao, S., Vepakomma, D., & D'Cruz, A. J. (2007). Bilateral spontaneous asymptomatic urinoma: report of an unusual case. Journal of Pediatric Urology, 3, 507-508.

• Tryfonas, G. J., Avtzoglou, P. P., Chaidos, C., Zioutis, J., Gavopoulos, S., & Thessaloniki, C. L. (1993). Renal hydatid disease: diagnosis and treatment. 28, 228-231.

• Kahriman, G., Ozcan, N., Dogan, S., & Bayram, A. (2016). Imaging findings and management of diaphragmatic mesothelial cysts in children. Pediatr Radiol.

• Seenu, V., Misra, M. C., Tiwari, S. C., Jain, R., & Chandrashekhar, C. (1994). Primary pelvic hydatid cyst presenting with obstructive uropathy and renal failure. Postgrad Med J, 70, 930-932.

• Czerwinska, K., Brzewski, M., Majkowska, Z., Mosior, T., Roszkowska- Blaim, M., & Warchof, S. (2014). The abdominoscrotal hydrocele in the infant- case report. Pol J Radiol, 79, 108-111.

• Doudt, A. D. F., Kehoe, J. E., Ignacio, R. C., & Christman, M. S. (2016). Abdominoscrotal hyrocele: a sistematic review. Journal of Pediatric Surgery.

• Casella, E., Giunta, G., Ventura, B., Cariola, M., Presti, L. L., Gallo, C., Tomaselli, C. F., Saphia, F., Comito, C., Castellano, L. M., Simone, G. D., & Caruso, S. (2003). Fetal megacystis: aetiology and management. Giorn. It. Ost. Gin. Giornale Italiano di Ostetricia e Ginecologia, 35, 669- 673.

• Kadian, Y. S., & Rattan, K. N. (2014). Congenital pyloric atresia with distal duodenal atresia: role of CT scan. J Neonatal Surg, 3, 37.

• Lockhart, M. E., Smith, J. K., & Kenney, P. J. (2002). Imaging of adrenal masses. Europian Journal of Radiology, 41, 95-112.

• Luks, F. I., Yazbeck, S., Homsy, Y., & Collin, P. P. (1993). The abdominoscrotal hydrocele. Eur J Pediatr Surg, 3, 176-178.

• Taghavi, K., Sharpe, C., & Stringer, M. D. (2017). Fetal megacystis: a systematic review. Journal of Pediatric Urology, 13, 7-15.

• Johnson, A. R., Ros, P. R., & Hjermstad, B. M. (1986). Tailgut cyst: diagnosis with CT and sonography. AJR, 147, 1309-1311.

• Schulman, M. H. (1999). Imaging of neonatal gastrointestinal obstruction. Radiologic Clinics of North America, 37, 1163-1186.

• Yang, D. M., Park, C. H., Jin, W., Chang, S. K., Kim, J. E., Choi, S. J., & Jung, D. H. (2005). Tailgut cyst: MRI evaluation. AJR, 184, 1519-1523.

• Kocaoglu, M., & Frush, D. P. (2006). Pediatric presacral masses. RadioGraphics, 26, 833-857.

• Ilce, Z., Erdogan, E., Kara, C., Celayir, S., Sarimurat, N., Senyuz, O. F., & Yeker, D. (2003). Pyloric atresia: 15-year review from a single instiution. Journal of Pediatric Surgery, 38, 1581-1584.

• Toma, P., Mengozzi, E., Acqua, A. D., Mattioli, G., Pierona, G., & Fabrizzi, G. (2002). Pyloric atresia: report of two cases. Pediatr Radiol, 32, 552-555.

ADVANCED DIAGNOSTIC MODALITIES AND MINIMALLY INVASIVE APPROACHES IN PEDIATRIC RADIOLOGY: A MULTIDISCIPLINARY REFERENCE